Towards Optimal Architectures for Hazard Monitoring Based on Sensor Networks and Crowdsensing

Didier Georges

IDRiM (2020) 10 (1) **ISSN: 2185-8322**
DOI10.5595/001c.xxxxxxx

Journal of Integrated Disaster Risk Management

Original paper

Towards Optimal Architectures for Hazard Monitoring Based on Sensor Networks and Crowdsensing

Didier Georges[1]

Received: 18/03/2020 / Accepted: 07/09/2020 / Published online: dd/10/2020

Abstract The monitoring of hazards through the ability to detect events and predict spatial and temporal evolution of dynamical hazards still remains a big challenge for dynamic disaster risk assessment and mitigation. The goal of this paper is to show how well established methods arising from the control theory can positively contribute to dynamic risk assessment improvement through an effective hazard monitoring. More precisely, the objective is threefold. Firstly, the design of an optimal monitoring architecture is proposed based on the combination of optimal sensor placement and receding horizon observer design. In this paper, the focus is only made on model-based and data-driven approaches. The benefit of using sensor networks and crowdsensing techniques is also discussed. Secondly, the paper seeks to identify the application areas that can benefit from both optimal sensor location techniques and receding horizon observers, while reviewing already existing references. Thirdly, some personal contributions illustrating the proposed approach are presented. In particular, two case studies are presented: one considers the dynamic positioning of drones for monitoring air pollution, the other is dedicated to the early detection of a wildfire outbreak.

Key words: Natural and technological hazard monitoring, optimal sensor location, receding horizon observer.

[1] Univ. Grenoble Alpes, CNRS, Grenoble INP*, GIPSA-lab, 38000 Grenoble, France
*Institute of Engineering & Management / Univ. Grenoble Alpes

1. INTRODUCTION*

The early detection and the ability to predict spatial and temporal evolution of natural or technological hazards still remain a big challenge for disaster risk assessment and mitigation [Zio (2018)]. Designing effective monitoring architectures for that purpose is of great concern for natural hazards such as landslides, earthquakes, flooding, wildfires, air pollution, for critical infrastructures [Alonso *et al* (2018)], such as power, gas, water, oil, traffic and transportation networks, for engineered structures of bridges, buildings and other related infrastructures submitted to various stresses (earthquakes, structural ageing, attacks), or for pandemic detection and prediction. Another big challenge in risk assessment is to be able to predict cascading effects when, for instance, a natural hazard triggers a technological disaster. The current covid-19 crisis shows that it is more necessary than ever to have numerical tools to predict the evolution of a crisis so as to be able to anticipate decision-making.

Nowadays the development of the Internet of Things increases the availability of various sources of spatio-temporal data, thanks to the design of more and more autonomous and miniaturized systems capable of self-powering and communicating, and increasingly dense and high-speed communications networks (see the current deployement of 5G technology). This allows the deployement of wireless sensor networks which are made up of embedded and spatially distributed sensors with communication capabilities. The development of unmanned aircraft systems (UAS) allows the sensor networks to become mobile and reconfigurable. In the same way, static or moving individuals carrying or using smartphones can be viewed as parts of a static or mobile wireless sensor network. The involvement of a large number of individuals which collectively share data and extract information is called crowdsensing [Capponi *et al* (2019)], [Zhang *et al* (2019)]. Some successful applications of crowdsensing or crowdsourcing based on social media data are now available: For instance, in the domain of seismic risk reduction and awareness [Bossu *et al* (2018)] with LastQuake app, and with the tuning of influenza spreading models using tweeter data [Levy *et al* (2018)] or, more recently, the development and use of mobile applications for the mapping of persons infected by the COVID-19.

In this paper, a model-based framework arising from control theory to design a monitoring architecture based on wireless sensor networks and crowdsensing for dynamical monitoring is discussed. The central idea is to design a digital architecture which is optimal in the sense that it ensures the best possible use of data provided by sensors in order to provide the most accurate online information about a dynamical hazard evolving in both space and time.

In this paper, a mathematical model of the phenemenon generating hazards is assumed to be available together with a set of static or mobile sensors providing on-line measurements. The proposed approach relies on two key components:

* This work is supported by the French National Research Agency in the framework of the Investissements d'Avenir program (ANR-15-IDEX-02). Parts of this work were presented at IDRIM 2019 International Conference, October 16-18, 2019, Nice, France and international conferences in Automatic Control without been published in any journal.

(1) Firstly, the optimal placement of sensors that can be either static [Georges (1995)], [Wouwer *et al* (2000)], [Ucinski (2005)], [Lou *et al* (2003)], [Kang *et al* (2011)], [Mallardo (2013)], [Spinelli *et al* (2017)], [Tang *et al* (2017)], or mobile [Demetriou (2008)], [Georges (2013a)], to ensure the best possible observation of the hazard to be monitored. In this paper, the problem of optimal sensor location is addressed using the so-called observability theory [Besançon (2007)]. It consists in maximizing a measure of the observability of some partial differential equations governing the spatial and temporal dynamics of physical hazards. Observability is the structural property of a system that makes it possible to estimate the current system state using only the information from outputs (measurements provided by sensors).

(2) Secondly, the design and use of an observer that is an algorithm used to process the distributed data delivered via sensor or crowd networking, whose goal is to detect unexpected events or to estimate or predict the spatial and temporal dynamics of the hazard. In this paper, the focus is made on the on-line model-based receding or moving horizon estimation algorithm [Michalska *et al* (1995)], [Muske *et al* (1995)], that can be viewed as the deterministic implementation of a nonlinear Bayesian filter allowing more flexibility (for instance to take constraints into account). It belongs to the class of model-based and data-driven state estimators such as Kalman filtering, extended Kalman filtering, unscented Kalman filtering, particle filtering, (see [Rawlings *et al* (2006)] for Kalman filter related approaches, and [Besançon (2007)] for other nonlinear state observer design).

The paper is organized as follows. In section 2, some background is provided on the central notion of dynamical system observability and a review of criteria providing a measure of observability is proposed. The formulation and solution of some optimal sensor location problems are discussed and a review of existing applications is provided. In section 3, the notions of both sensor networks and crowdsensing are presented and a discussion is provided on how to use these techniques for hazard monitoring. Section 4 is devoted to receding horizon observer design. Both the formulation and solution of the related optimization problem are also discussed. In section 5, an optimal architecture design based on the combination of both optimal sensor location and receding horizon observer techniques is presented. Section 6 considers two case studies -the dynamic positioning of drones for monitoring air pollution, and the early detection of a wildfire outbreak- to illustrate the proposed framework. Finally, the last section sums up the conclusions and perspectives.

2. OBSERVABILITY, OPTIMAL PLACEMENT OF SENSORS OR HOW TO INCREASE MONITORING CAPABILITIES

Monitoring of spatio-temporal dynamical systems consists in processing various data collected through time and space to estimate the past and current parameters or states of the system. Based on the estimation of future events or inputs affecting the system, monitoring may also allow the prediction of the spatio-temporal dynamics of the system. Monitoring of

large-scale dynamical systems is a big challenge for risk management and safety since it provides a way to isolate or estimate system vulnerabilities or the occurence and evolution of a (natural or man-made) hazard. In this paper, we will focus on model-based approaches, i.e., approaches requiring the a priori knowledge of the mathematical representation of the system dynamics. In system control theory and physics, modelling is based on state-space representation (those properties have been studied by Kalman for linear systems, see [Ogata (2010)] for an introduction to linear control theory) or partial differential equations (PDEs) for spacetime distributed systems. Most of the applications are governed by PDEs and complex networks that require high level of computational complexity. However in many cases PDEs or networks can be well approximated using finite-dimensional state-space representations via model reduction techniques.

The major property required for the successful monitoring of a dynamical system is *Observability*, i.e. basically *the ability to recover the initial state of the system through the knowledge of some output measurements (obtained from sensors) collected over a time interval.*

Mathematically, Observability is defined *as the injectivity of the operator initial state to output, that can be also reformulated as the preservation of initial state distinctness or the nonzero output sensitivity to initial state (see [Besançon (2007)]* for more details).

$$y_1(t, x_1(t_0)) = y_2(t, x_2(t_0)), \forall t \in [t_0, t_0 + T] \Rightarrow x_1(t_0) = x_2(t_0) \quad (1)$$

In the case of parameters estimation, there is a related notion: *The Identifiability of parameters* θ:

$$y_1(t, \theta_1) = y_2(t, \theta_2) \Rightarrow \theta_1 = \theta_2. \quad (2)$$

This fundamental property opens the way to the development of algorithms for reconstructing the initial state of a system from measurements obtained over a time interval.

2.1 Measuring the degree of observability

The effective model-based monitoring requires optimal configuration of a limited number of sensors to ensure the best possible state/parameter estimation. *The Optimal Placement of Sensors* will here consist in seeking an optimal configuration of a fixed number of sensors in order *to maximize a measure of Observability/Identifiability*.

Gramian-based measures of Linear System Observability

Consider the class of linear finite-dimensional systems defined by the following linear state-space representation :

$$\begin{aligned} \dot{x}(t) &= Ax(t), x \in \mathbb{R}^N, x(0) = x_0, \\ y(t) &= Cx(t), y \in \mathbb{R}^P \end{aligned} \quad (3)$$

where *x* is the state, *y* is the output vector corresponding to measurements obtained by sensors.

If the measurement vector $y(t)$ is known over time interval $[0,T]$, the so-called *Output Energy generated by any initial state* x_0 is given by

$$E_0 = \int_0^T y^T(t)y(t)dt = x_0^T \{ \int_0^T e^{A^T t} C^T C e^{At} dt \} x_0 \quad (4)$$

since $y(t)=Ce^{At}x_0$. nonnegative-definite symmetric matrix $W(T)= \int_0^T e^{A^T t} C^T C e^{At} dt$, called *the Observability Gramian*, can be isolated (see also for instance [Kailath (1980)]).

$W(T) = W^T(T) \geq 0$ can be obtained as solution of the following differential Lyapunov equation:

$$\dot{W}(t) = A^T W(t) + W(t)A + C^T C, W(0) = 0. \quad (5)$$

This approach was extended to the case of algebraic-differential (singular) systems in [Marx *et al* (2004)].

It appears that $W(T)$ *is a measure of the sensitivity of output y with respect to initial state* x_0 (which can be interpreted as a Fisher Information Matrix (FIM) (see [Ucinski (2005)], and [Song *et al* (2009)] for interpretation of FIM): Indeed, the sensitivity of state $x(t)$ with respect to x_0 is given by

$$\frac{d}{dt}(\partial_{x_0} x(t)) = A\partial_{x_0} x(t), \partial_{x_0} x(0) = I_d \quad (6)$$

$$\partial_{x_0} y(t) = C\partial_{x_0} x(t) \Rightarrow \partial_{x_0} y(\mathrm{t}) = Ce^{A_t} \quad (7)$$

Then

$$\int_0^T \partial_{x_0} y^T(t)\partial_{x_0} y(t)dt = \int_0^T e^{A^T t} C^T C e^{At} dt = W(T), \quad (8)$$

where $\partial_{x_0} x(t)$ denotes the Jacobian matrix of partial derivatives $\frac{\partial x_i}{\partial x_{0j}}$.

The observability gramian is therefore a mathematical way to characterize the sensitivity of the system outputs to any initial state x_0, allowing the development of a methodology to optimally locate sensors. Another interesting feature is that the notion of observability gramians can be extended to the case of nonlinear systems.

Extension of observability gramians to Nonlinear Systems

Consider systems described by the following nonlinear state-space representation

$$\dot{x} = F(x,t,\theta),\ x \in \mathbb{R}^N,\ x(0) = x_0, \quad (9)$$
$$y = H(x,t),\ y \in \mathbb{R}^P,$$

where x denotes the state vector, y, the output vector, and θ, the vector of model parameters, and F is supposed to continuously differentiable.

Again the application of the sensitivity analysis is possible, which leads to the following sensitivity equations:

$$\frac{d}{dt}(\partial_{x_0}x) = \partial_x F(x,t,\theta)\,\partial_{x_0}x, \partial_{x_0}x(0) = I_d\,, \tag{10}$$

$$\partial_{x_0}y = \partial_x H(x,t)\,\partial_{x_0}x\,;\, \dot{x}\,F = (x.t) \tag{11}$$

Formally *the nonlinear Observability Gramian* can be defined by:

$$w(x_0,T) = \int_0^T \partial_{x_0} y^T(t)\partial_{x_0}y(t)dt. \tag{12}$$

It is worth noticing that the linear observability gramian defined by (8) appears to be a special case of this general formalism. However the gramian depends on initial state x_0 in the nonlinear case.

It is also worth mentioning that a similar approach can be used to study parameter identifiability by introducing the sensitivity of the state with respect to the vector of system parameters θ:

$$\frac{d}{dt}(\partial_{\theta x}) = \partial_x F(x,t,\theta)\,\partial_\theta x + \partial_\theta F(x,t,\theta), \partial_\theta x(0) = 0, \tag{13}$$

$$\partial_\theta y = \partial_x H(x,t)\,\partial_\theta x\,;\dot{x} = F(x,t,\theta). \tag{14}$$

Then *the nonlinear Identifiability Gramian* can be defined by:

$$W(\theta,T) = \int_0^T \partial_\theta y^T(t)\partial_\theta y(t)dt. \tag{15}$$

In practice, the computation of sensitivity equations (10)-(11) or (13)-(14) can be highly complex, especially for systems with a large number of states or parameters. Indeed, a *N*-dimensional system with *M* parameters to identify (or *N* initial states to estimate), requires the integration of a sensitivity system in a space of dimension $N\times M$ (or N^2). To overcome this drawback, empirical computation of the observability gramian has been proposed that requires only simple simulations of the system.

Empirical observability gramian [Lall *et al* (1999)]

The empirical gramian is obtained by applying some small pertubations to each component of the initial state and performing time integrations to get the output trajectory corresponding to each perturbated initial state. For (nonlinear) dynamical systems, the empirical observability Gramian can be defined as

$$W = \sum_{l=1}^{r}\sum_{m=1}^{s}\frac{1}{rsc_m^2}\int_0^T T_l \Psi^{ilm}(t)T_l^T\,dt$$

where $\Psi^{lm}(t) \in \mathbb{R}^{N\times N}$ is given by $\Psi_{ij}^{lm}(t) = \left(y^{ilm}(t) - y^{ilm,0}\right)^T \left(y^{ilm}(t) - y^{ilm,0}\right)$, and y^{ilm} is the output obtained with perturbated initial condition $c_m T_l e_i + x_0$, and $y^{ilm,0}$ refers to the output obtained with unperturbated initial state x_0; T_l is a perturbation direction, and e_i is a standard unit vector in $\mathbb{R}^N$. For more details, the reader is invited to refer to [Lall *et al* (1999)].

Some other approaches for the characterization of system observability

The observability gramian-based approach is not the only way quantify observability. Other observability indices may be derived by using the injectivity property (an observability inequality) that can be reformulated as follows:

The system $\dot{x} = F(x,t)$, $y = H(x, t)$ is observable in time T if there exists $C > 0$ such that

$$C\|x_1(0) - x_2(0)\|^2 \leq \int_0^T \|y(t, x_1(0)) - y(t, x_2(0))\|^2 dt \tag{16}$$

for any pair of initial state $(x_1(0), x_2(0))$ in the estimation space (included in the state space). Here $y(t,x(0))$ denotes the system output generated by initial state $x(0)$.

A similar observability inequality can be formulated when dealing with partial differential equations (see for instance Privat *et al.* (2014)).

The authors in King *et al.* (2014) proposes to exploit this definition by defining an unobservability index as follows:

$$\varepsilon^2 = \min_{\delta x_0} \delta X_0^T P_1 \delta X_0 + \int_0^T \|y(t, X_0 + \delta X_0) - y(t, X_0)\|_{P_2}^2 \, dt \tag{17}$$
$$s.t. \|\delta X_0\| = \rho, \delta X_0 \in W$$

where W is the estimation space, and P_1 and P_2 are weighting matrices. The ratio $\frac{\rho}{\varepsilon(\mu)}$ denotes the unobservability index. A good observability is obtained when the ratio is minimal, i.e, when ε is maximal.

One can also directly work on the performance of state observers or data assimilation problems by considering the state estimation error, for instance, using the Kalman filter (see [Tang *et al* (2017)] for a description of this approach in the infinite dimensional framework), based on the covariance matrix P of the observation error defined by

$$trace[P] = trace[E\{(x-\hat{x})\,(x-\hat{x})^T)\}], \tag{18}$$

where P is the non negative-definite symmetric matrix, solution of Kalman filter stationary Riccati equation

$$AP + PA^T - PC^T R^{-1} CP + Q = 0. \tag{19}$$

One of the three metrics (20), (21), or (22) can be used with covariance matrix P to measure the degree of observability.

A similar approach based on a norm of the state estimation error, is used for instance in Demetriou (2008) for the location of a mobile sensor and in Lou *et al.* (2003) for the optimal sensor location of a system governed by a nonlinear partial differential equation. For data assimilation problems, a similar approach is also proposed in Herzog *et al* (2017).

For Riesz-spectral linear partial differential equations or finite-dimensional systems, eigenvalue/eigenfunction decomposition allows to use the modal components of the measurement/output operator to measure the degree of observability (see section 6.1.2). This kind of approach is used in structural health monitoring (see [Mallardo (2013)] that also provides an extensive review of optimal sensor locations techniques.

Frequency-based approaches have been also proposed (see [Demetriou *et al* (2014)]) that exploit the spatial H_2 norm of the transfert function of a 1D diffusion-advection partial differential equation. The spatial H_2 norm can be used as a measure of sensor sensitivity over the spatial domain.

The question is now to examine how observability gramians / FIM or other approaches can be used to design an appropriate observability metric, usable as a cost function for solving an optimal sensor location problem.

2.2 Observability gramian-based cost functions for optimal sensor placement

Three classical metrics based on the spectral analysis of observability gramian / FIM $W(T,\mu)$, where μ is a given sensor configuration corresponding to specific choices of state measurements or physical locations of the sensors are here recalled (see also [Herzog *et al* (2017)]):

$$c(\mu) = trace(\mathrm{W}(T,\mu)) = \sum_{i=1}^{N} \lambda_i(\mu), \tag{20}$$

$$c(\mu) = (\log) det\big(W(T,\mu)\big) = (\log) \prod_{i=1}^{N} \lambda i\,(\mu), \tag{21}$$

$$c(\mu) = \underline{\lambda}\big(W(T,\mu)\big) = \min_{i=1,\ldots,N} \lambda_i(\mu), \tag{22}$$

where the λ_i's, $i = 1,\ldots,N$, denote the eigenvalues of symmetric (N,N)-matrix $W(T,\mu)$.

The trace of the observability gramian (20) does not guarantee full observability, since some eigenvalues of W can be equal to zero. These null eigenvalues correspond to non observable state components. However, for exponentially stable systems, at least detectability (a weak form of observability where at least one stable state component is non observable) is ensured, meaning that asymptotic observers (such as Kalman filters) will converge. This metric only tends to improve observability of the dominant modes of the system. If metric (20) is used as a cost function to be maximized, an optimal sensor configuration achieves the maximum observability in average.

In contrast, stricly positive values of metrics (21) and (22) guarantee that all the state components are observable.

2.3 Other cost functions for optimal sensor placement

ε^2 given by (17) can be used as a cost function $c(\mu)$, solution of a minimization problem, if one considers parametrization of the measurement operator C in function of sensor location μ:

$$c(\mu) = \varepsilon^2(\mu) = \min_{\delta X_0} \delta X_0^T P_1 \delta X_0 + \int_0^T \|y(t, X_0 + \delta X_0, \mu) - y(t, X_0, \mu))\|_{P_2}^2 dt \qquad (23)$$
$$s.t. \|\delta X_0\| = \rho, \delta X_0 \in W$$

Notice that the use of the cost function will lead to the solution of max-min optimization problem.

In the same way, (18) defines a cost function $c(\mu)$, whose computation is obtained by solving the following algebraic equation parametrized in μ:

$$AP(\mu) + P(\mu)A^T - P(\mu)C^T(\mu)R^{-1}C(\mu)P(\mu) + Q = 0. \qquad (24)$$

For data assimilation problems, a similar approach is also proposed in [Herzog *et al* (2017)].

2.4 Formulation of an optimal sensor location problem OSPP

It is now possible to define a generic Optimal Sensor Placement Problem OSPP which consists in maximizing one of the presented observability metrics:

$$\max_{\mu \in \mathcal{D}_\mu} c(\mu), \qquad (25)$$

where $\mathcal{D}_\mu$ defines a set of constraints such as density constraints, communication range constraints, placement constraints . OSPP is usually a non convex optimization problem. Also notice that index (22) is not differentiable, leading to additional complexity that can be overcome by using subgradient optimization techniques [Bertsekas (2015)], [Karmitsa (2016)].

Solving OSPP can be a complex task especially for large-scale systems and in the case of sensors configurations constrained to belong to a set of discrete values (defining an integer programming problem). This is for instance the case when the OSSP consists in determining the location of a set of sensors. A big issue is the so-called curse of dimensionality since OSPP usually relies on exponential N^2-complexity computations where N is the dimension of the system state space. In order to limit this complexity, model-reduction techniques have been proposed for large-scale systems (especially systems governed by partial differential equations), see for example, [Antoulas *et al.* (2006)] for large-scale finite-dimensional systems or [Benner *et al* (2017)] for systems governed by partial differential equations. Furthermore, a mixed integer programming OSPP has to deal with combinatorial explosion. The interested reader is

invited to refer to appropriate references such as [Burer *et al* (2012)] which discuss the algorithmic techniques available to overcome the limitations due to combinatorial complexity.

In many situations, it is important to adapt the locations of the sensors, especially when the dynamics of the monitored phenomenon is time-varying (for instance, air pollution or wildfires with changing meteorological conditions). The OSPP for *M* mobile sensors can be formulated as an optimal control problem, where the dynamics of the mobile sensors can be also taken into account together with energy consumption:

$$\min_{u_i(t)} \sum_{i=1}^{M} \int_0^T \underbrace{[z_i^T(t)Qz_i(t) + u_i^T(t)Ru_i(t)]}_{\textit{energy consumption}}\, dt - \underbrace{c(\mu_1(T), \dots, \mu_M(T))}_{\textit{observability index}} \tag{26}$$

subject to

$$\dot{z}_i(t) = G_i\big(z_i(t), u_i(t)\big), i = 1, \dots, M, \tag{27}$$

$$\alpha \le d_{ij}(t) \le \beta, i = 1, \dots, M-1,\ j = i+1, \dots, M, \tag{28}$$

where $z_i = (\mu_i(t), \dot{\mu}_i(t))^T$ denotes the position and velocity of sensor *i* at time *t*. $u_i(t)$ is the navigation control input of sensor *i*. *Q* and *R* are weighting matrices. $d_{ij} = \|\mu_i(t) - \mu_j(t)\|_2$ is the euclidian distance between sensor *i* and sensor *j*. (27) represents the state-space equations of the dynamics of sensor *i*. Inequality constraints (28) are introduced for mutual collision avoidance purpose and mutual communications.

Provided that cost function *c* is differentiable, a less demanding navigation approach is the kinematic approach (i.e., without introducing the sensor dynamics, see for instance [Georges (2013a)]) may consist in using a gradient-based method of the form:

$$\dot{\mu}_i(t) = \rho[\nabla_{\mu i} c(\mu_1(t), \dots, \mu_M(t)) + \delta \sum_{j=1,\ j\neq i}^{M} \{\frac{(\mu_i(t) - \mu_j(t))}{d_{ij}^2(t) - \alpha^2} - \frac{(\mu_i(t) - \mu_j(t))}{\beta^2 - d_{ij}^2}\}], \rho, \delta > 0. \tag{29}$$

The trajectory of each sensor *i* follows the direction imposed by the gradient of $c(\mu_1(t), \dots, \mu_M(t)) + \delta \sum_{i=1,}^{M-1} \sum_{j=i+1}^{M} \{\log(d_{ij}^2 - \alpha^2) + \log(\beta^2 - d_{ij}^2)\}$ with respect to μ_i, where $\sum_{i=1,}^{M-1} \sum_{j=i+1}^{M} \{\log(d_{ij}^2 - \alpha^2) + \log(\beta^2 - d_{ij}^2)\}$ are the sum of barrier functions (that can be viewed as repulsive potentials) introduced to avoid mutual collisions and ensure maximal interdistance. ρ controls the velocity and δ is a weighting coefficient used to adjust the importance of mutual avoidance constraints.

In fact, (29) can be viewed as a gradient method used for solving the maximization problem

$$\max_{\mu_1, \dots, \mu_M} c(\mu_1, \dots, \mu_M) + \delta \sum_{i=1,}^{M-1} \sum_{j=i+1}^{M} \{\log(d_{ij}^2 - \alpha^2) + \log(\beta^2 - d_{ij}^2)\} \tag{30}$$

In [Demetriou (2010)], an approach based on Lyapunov stability arguments is proposed to control collocated actuator-sensor mobile networks for improving control and estimation of systems governed by diffusion partial differential equations.

2.5 Some existing OSPP applications

Table 1 provides some already implemented examples of (OSSP) for hazard monitoring.

Table 1. Applications of OSPP for Hazard Monitoring.

Hazard	Sensors	Some References
Weather	meteorological stations, satellites, crowdsensing	[Demetriou *et al* (2014)]
Overland or urban flooding	water level or flow rate sensors	[King *et al* (2014)], [Nguyen *et al* (2016)], [Ogie *et al* (2017)], [Park *et al* (2017)]
Landslides, avalanches, lava flows, mudflows	LIDAR, satellite, stress sensors, crowdsensing	[Terzis *et al* (2006)], [Thuro *et al* (2017)]
Pollution	pollutant sensors, crowdsensing	[Georges (2011)], [Georges (2013a)], [Georges (2013b)], [Boubrima *et al* (2015)]), [Kouichi *et al* (2016)]) [Georges (2017)])
Epidemics and pandemics (including rumor propagation)	crowdsensing, hospitals and medical centers	[Spinelli *et al* (2017)]
Critical infrastructures (water, gas, oil, energy, traffic flow networks), industrial facilities or processes, buildings …	physical sensors depending on the infrastructure, crowdsensing	[Nguyen *et al* (2008)], [Mallardo (2013)], [Georges (2014)], [Qi *et al* (2014)], [Casillas *et al* (2015)], [Herzog *et al* (2017)], [Khorshidi *et al* (2018)], [Summers *et al* (2014)], [Zan *et al* (2018)]

3. SENSOR NETWORKS AND CROWDSENSING

A Wireless Sensor Network (WSN) is a set of embedded sensors, spatially disseminated, able to use wireless communications with each other and to send data to a sink station (see Fig. 1). The WSNs are used to collect physical data, such as temperature, sound, pollution

concentrations, humidity, wind velocities, and so on. The WSNs offer several interesting features, such as flexibility (no expensive infrastructure is required) and measurement redundancy offering more robustness to node failures. However they are often subject to power consumption constraints, except if they are equipped with energy harvesting devices. For a recent survey, see [Mostafaeia *et al* (2018)].

Some WSNs can be mobile. However in this case, the management is much more complex since the sensors have to be coordinated in order to ensure connectivity and the energy management of the sensors is also more demanding. Navigation approaches (26) or (29) are some examples of techniques that can be used to coordinate mobile sensor networks.

Crowdsensing is a technique where a group of individuals uses mobile or static devices capable of sensing and providing qualitative or quantitative data (see Fig 2 and [Capponi *et al* (2019)]). Today most smartphones are equipped with sensors such as cameras, microphones, GPS and accelerometers, temperature sensors, which can be used to provide quantitative data, for example to detect or locate earthquakes or to monitor traffic congestion in real time.

Crowdsensing can be classified into two classes: the opportunistic crowdsensing, where the data is collected without user intervention via specialized samrtphone applications, and the participatory crowdsensing, where many users voluntarily provide information through social networks or specialized applications. Both approaches can give access in addition to a huge number of qualitative data, which can be very relevant to reinforce physical knowledge in vulnerability or hazards after adequate processing. Or course, crowdsensing (even in the participatory case) is less suitable for the implementation of observability maximisation techniques such as (25), as it can be difficult or even dangerous to ask a large number of people to position themselves in order to increase the observability of a natural hazard (such as a flood or a forest fire). However, this defect can be compensated by the fact that the number of sensors is potentially higher and the coverage is therefore potentially wider.

Advances in Artificial Intelligence offer highly effective machine learning techniques for extracting quantitative data from qualitative data (for the goal of pattern recognition and classification for instance) (see [Zhang *et al* (2019)] for a recent survey).

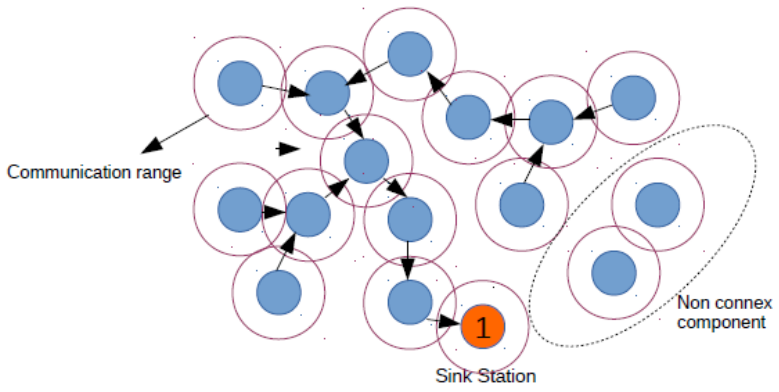

Figure 1. WSN structure - each node in blue is a wireless sensor. Some unconnected part of the WSN may exist. The communication range is limited and here depicted by a circle.

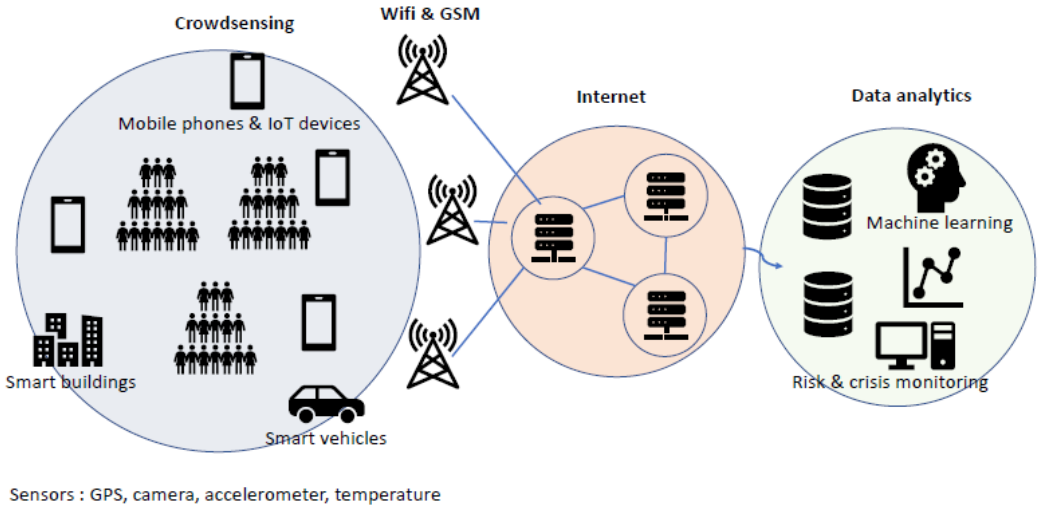

Figure 2. Crowdsensing (see also Alsheikh (2017)).

Participatory crowdsensing can be very useful in providing information about hazard magnitude and location during an extreme weather event, flooding, earthquakes, or epidemics for example. A description of the process with illustrative examples is given by Fig. 3. The learning process relies on the availability of data sets obtained from past events or simulations. The data sets are used to learn a regression/classification model that will provide an estimate of the magnitude of an event occurring at a given time instant together with a degree of confidence. The processed data (estimated value + degree of confidence) then can be used for model-based monitoring as depicted in the section here-after.

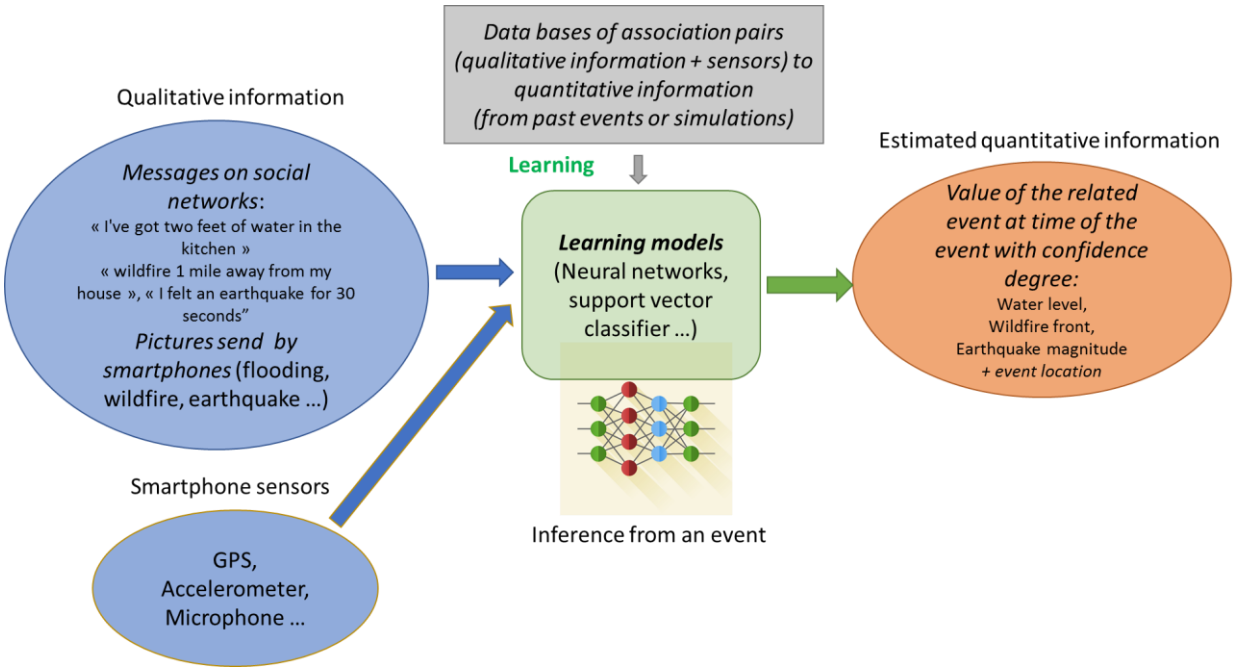

Figure 3. From qualitative to quantitative data through machine learning.

4. RECEDING HORIZON OBSERVERS FOR DYNAMIC HAZARD ASSESSMENT AND REAL-TIME MONITORING: AN OPTIMIZATION APPROACH

In this section, some background is provided on Receding or Moving Horizon Observer design. The main goal is to show how this approach can be useful to ensure real-time monitoring of an evolving hazard or to estimate vulnerability.

Hazard monitoring must be here understood as the online process described by Fig. 4 that consists in processing data provided by a large number of sensors on a time period $[t_k - T, t_k]$, called receding or moving horizon, at each sampling time denoted as $t_k = kT_s$, where T_s is the sampling period, in order to get estimate of both system state at $t_k - T$ and unknown system parameters. It is worth noticing that *this approach does not necessarily require a large and dense coverage with sensors to get relevant spatio-temporal information, thanks to the observability property.*

In this paper, one considers that the phenomenon to be monitored is described by the following nonlinear state-space representation

$$\begin{aligned} &\dot{z}(t) = F(z(t), u(t), \theta), z(t) \in \mathbb{R}^n, z(0) = z_0, u \in \mathbb{R}^m \\ &y(t) = H(z(t), t), y(t) \in \mathbb{R}^p, \end{aligned} \tag{31}$$

where $z(t)$ denotes the state vector, u is the vector of known exogenous inputs, y is the vector of measured outputs provided by the sensors, and θ is the vector of unknown parameters.

If the phenomenon is governed by partial differential equations, spatial discretization on a grid or model reduction techniques have to be performed in order to get form (31). In the case of systems governed by partial differential equations (PDEs), such as floods governed by the shallow water equations, pollution governed by several diffusion-advection-reaction PDEs or earthquake dynamics governed by 3D elastic wave equations for instance, the dimension of the state space can be very large. A big challenge in current research is to develop effective low-dimensional model reduction techniques (see [Benner *et al* (2017)] for a review of techniques as Proper Orthogonal Decomposition (POD), balanced truncation, tensor-based approaches).

The measurements are assumed to be obtained from physical sensors or from qualitative information provided by individuals via the social media (through crowdsensing), with a certain degree of confidence (see Fig. 3). θ can represent either physical parameters (such physical diffusion or source location) or information on particular dysfonctionning or failures in the case of critical infrastructures. The reader is invited to refer to Table 3 for concrete examples of what are state variables and parameters for various hazards.

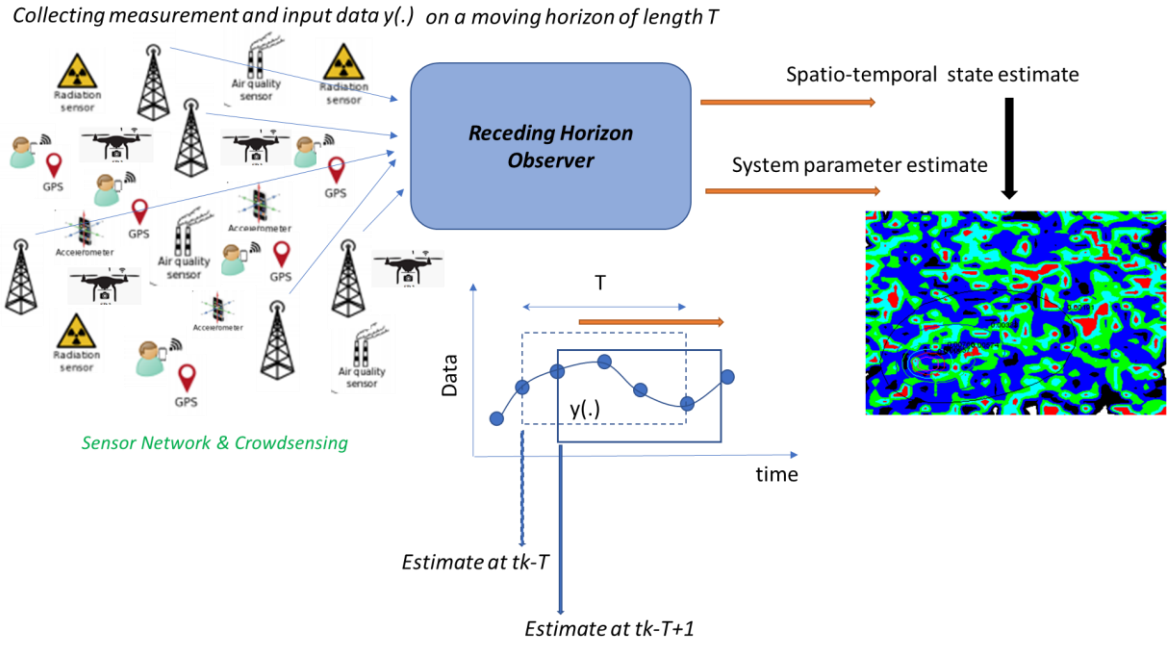

Figure 4. Principle of RHO with sensor network and crowdsensing.

4.1 The receding or moving horizon observer formulation

The following notation will be used in what follows to denote the forward solution of (31) at time τ, starting from state z at time t:

$$Z(\tau, z, u(.), \theta), \tau \geq t. \tag{32}$$

State and/or Parameter Receding or Moving Horizon Observers RHO (see [Michalska *et al* (1995)], [Muske *et al* (1995)], [Kuhl *et al* (2011)], [Rangegowda *et al* (2018)]) provide an estimate of both x and θ of the true x and θ by minimizing the output prediction error in the least-square sense over a past receding horizon defined by horizon T, at each time t_k:

$$\{\hat{z}(t_k - T), \hat{\theta}_k\} = arg \min_{z \in \mathfrak{Z}(t), \theta \in \Theta} \int_{t_k - T}^{t_k} \| y(\tau) - H(Z(\tau, z, u(.), \theta), \tau) \|^2_{R^{-1}} d\tau + \| z - \bar{z} \|^2_{M_1^{-1}} + \| \theta - \bar{\theta} \|^2_{M_2^{-1}}, \tag{33}$$

where $y(t)$ denotes the measured data at time t, weighting matrix R can be interpreted as the covariance matrix of a noise vector affecting the output measurement. H denotes the measurement operatr R^{-1} can also be used to reflect the degree of confidence in the measurements (particularly useful for data obtained from crowdsensing). R^{-1} can also depend on time to introduce some forgetting factor with respect to past measurements. M_1 and M_2 can be viewed as regularization matrices or the covariance matrices of uncertain variables z and θ. $\mathfrak{Z}(t)$ is the set of admissible values of the state at time τ (often the set is used to impose the state remains positive, for instance, in the case of physical densities). Θ is the set of admissible values of the parameters. $\bar{z}$ and $\bar{\theta}$ are guess values of initial state z ($t_k - T$) and θ respectively, for instance estimated values obtained from the algorithm at previous sample time $t_k - T - 1$.

It is worth mentioning that (33) provides in fact an estimate of state z at time $t \in [t_k - \mathrm{T}, t_k + 1]$, since it suffices to integrate (31) from estimate state $\hat{z}(t_k - T)$, knowing $u(.)$ and the estimate of θ.

4.2 Relevance of the RHO approach

The main value of RHO lies in the fact that each new sample of the sensor measurements are used to provide an update of the state estimate thanks to the online solving of (33).

Measurement reliability is a big concern especially when low cost sensors are used in sensor networks, since indeed they can be prone to failure or lack of precision. The interest of using model-based estimation/filtering whose effectiveness relies on the fundamental property of observability, is the fact that estimation algorithms, such as the receding horizon which is based on optimal filtering, are able to provide estimates of the distributed states based on a limited number of well-placed sensor measurements which can be subject to measurements noise. Thus the covariance matrix of the measurement noise is explicitely taken into account in the minimized cost function (see eqn (33)), where R denotes the covariance matrix of noises affecting the sensors).

This approach also provides a lot of flexibility allowing inclusion of heterogeneous, sporadic or asynchronous data produced by static or mobile sensors, especially in the context of crowdsensing. In this case, the number of sensors can actually vary considerably over time. Think about the increasing number of posts in social media observed during a disaster. Furthermore, taking measurements delays due to limited transmission rates in some sensor network configurations, is important if the monitored dynamics has ”small time constants” with respect to the measurement delays. The development of 5G technologies will soon make the problem of delayed data obsolete due to the gain in transmission rates (x10 compared to 4G). However, it is worth mentioning that there exist well-established results on the estimation of systems time-delayed measurements and data loss [Johansen *et al* (2013)]. Formulation (33) can be modified to include delayed data. However the computation of the optimization is more tricky. Finally, extension of the RHO have been proposed to hybrid dynamical systems [Ferrari *et al* (2003)]. A hybrid system is a dynamical system that exhibits both continuous and discrete dynamic behavior, i.e. a system that combines both differential equations and discrete event automatons. The class of hybrid systems has to be considered with attention when dealing with cascading hazards such as natural hazards triggering technological disasters (Natech risks). It is worth noticing that such flexibility cannot be obtained using the Kalman filtering approach -and its variants- that cannot include constraints in particular in the estimation process.

It can be shown that the existence of a solution to (33) relies on both the state observability and parameter identifiability properties of system (31). Improving observability/identifiability by solving an OSPP (25) will increase the sensitivity of output measurements $y(\tau), \tau \in [t_k - T, t_k]$ to state $z(t_k)$ which generated them. It can be shown that such sensitivity computations are involved in solving (33), for instance through the computation of an adjoint model.

Solving optimal problem (33) usually requires the computation of a large scale optimization problem in particular when dealing with discretized PDEs with a large number of state variables. Again the use of model reduction techniques is a key factor for reducing computational complexity. In addtion, efficient solvers have been developed over the last decades to solve large-scale constrained optimization problems, such as solvers based on sequential quadratic programming techniques associated to quasi-Newton methods [Gould *et al* (2005)] or Limited Memory Bundle Methods for solving large-scale nonsmooth optimization problems [Karmitsa (2016)].

Due to its ability to cope with constraints and its intrinsic flexibility in the formulation, some particular formulations of RHO can be viewed as the generalization of Kalman filter that hold only for linear unconstrained systems subject to Gaussian noises. (see [Alamir (2007)]) .

4.3 Review of some existing or potential RHO applications

RHO implementations are still limited in environmental applications, despite the flexibility of the approach. However, many data assimilation techniques and Kalman filter variants have been developed in the literature, that are not reviewed here. However successful implementations of RHO are available in the literature related to the monitoring of industrial processes or facilities, that are listed here.

Table 2 provides some potential applications of RHO techniques for hazard monitoring.

5. OPTIMAL MONITORING ARCHITECTURE

In this section, the overall optimal architecture proposed in the paper is described and formalized.

Some additional notations are introduced.

The measurement operator related to static sensors and the locations of the static sensors are denoted as $y_s(t) = C_s(\mu_s)z(t), y_s \in \mathbb{R}^{N_s}$ and μ_s respectively, where N_s is the number of static sensors.

- The measurement operator related to controlled mobile sensors, such as UAVs, and the time-varying locations of these mobile sensors are denoted as $y_m(t) = C_m(\mu_m(t))\ z\ (t)$, $y_s \in \mathbb{R}^{N_m}$ and $\mu_m(t)$, respectively, where N_m is the number of mobile sensors.
- The measurement operator related to crowd sensors (individuals carrying smartphones), and the time-varying locations of these crowd sensors are denoted as $y_c(t) = C_c(\mu_c(t))$ z(t), $y_c \in \mathbb{R}^{N_c}$ and $\mu_c(t)$, respectively, where N_c is the number of crowd sensors.

Table 2. Potential or Existing Applications of RHO

Hazard	States	Parameters	Sensors	References
Weather	temperature, wind velocities, pressure fields …	extreme events	meteorogical stations, satellites, crowdsensing	
Overland or urban flooding	water levels, flow velocity in time and space	friction coefficient, location of dyke failures	water level or flow rate sensors	[Pham *et al* (2013)]
Landslides, avalanches, lava flows, mudflows	flow thickness , flow velocity, in time and space	friction and stress coefficients	LIDAR, satellite, stress sensors, crowdsensing	
Earthquakes	displacement and stress tensor, in time and space	Lamé elastic constants, density of the elastic medium, seismic source location	seismometers, crowdsensing	
Wildfire	Temperature, fuel consumption in time and space	diffusion and reaction coefficients, ignition location	infra-red sensors, crowdsensing, satellite	See section 6.2
Pollution	pollutant concentration in time and space	diffusion and reaction coefficients, pollutant source location	pollutant sensors, crowdsensing	
Epidemics and pandemics	susceptible, infected, recovered individual density in time and space	disease diffusion, infection, recovery rate coefficients	crowdsensing, hospitals and medical centers	
Ecology (Predator/Prey models)	predators and prey density in time and space	diffusion and rate of increase and competition coefficients	biological field stations	
Critical infrastructures (water, gas, oil, energy, traffic flow networks), industrial facilities or processes, buildings ...	flows and physical potentials	fault detection and isolation	physical sensors depending on the infrastructure, crowdsensing	[Alamir *et al* (2003)], [Mohd Ali *et al* (2015)], [Rangegowda *et al* (2018)]

When one considers systems governed by PDEs, the individual measurement operator C_i^j, i= *s*,*m*,*c*, for any sensor j is defined as follows:

$$C_i^j(\mu_i^j z\,(t)\;=\int_{\Omega_i}\Delta\,(\zeta,\mu_i^j)\;z(\zeta,t)d\,\zeta\,, \tag{34}$$

where $\Delta\,(\zeta,\mu_i^j)$ is the characteristic of a spatially averaged measurement around location μ_i^j

on domain Ω_i. Δ is often chosen as $\begin{cases} 1, if\ \zeta \in [\mu_i - \varepsilon, \mu_i + \varepsilon], \\ 0, otherwise \end{cases}$

The way of deriving the optimal location of sensors depends on the nature of the sensors:

- For static sensor units, the OSPP is solved once and for all.
- For controlled mobile sensing units, an adaptive OSPP is implemented where the observability index is updated at each sample time t_k using both state $\hat{z}(t_k-T-1)$ and exogeneous inputs on horizon $(t_k-T-1,t_k-1]$ -for instance, weather forecasting information: wind velocity, temperature, pressure- or control inputs performed on the system -for instance, actions of fire fighting units in the case of wildfires- and estimated parameters provided by the RHO, and the sensor trajectories are updated accordingly.
- For crowdsensing units, usually the OSPP does not make sense since the individuals freely evolve on the field. However if parts of the individuals (in the context of participatory crowssensing) accept to follow some prescribed trajectories in order to position themselves in order to maximize observability, they are assumed to belong to the category of controlled mobile sensors defined just before.

Based on (25), (29), (33), additional notations and previous assumptions, the overall iterative monitoring architecture can be formulated as follows:

Offline static OSP:

$$\max_{\mu_s \in D_{\mu_s}} c_s(\mu_s), \tag{35}$$

Mobile OSPP[2] updated at each t_k, starting from $\mu_m^i(t_k-1)$:

$$\dot{\mu}_m^i(t) = \rho[\nabla_{\mu_m^i} c_m(\mu_m^1(t),\dots,\mu_m^M(t), \hat{\theta}_{k-1}, \hat{z}(t_k-T-1), u([t_k-T-1,t_k-1])) + \delta \sum_{j=1,\ j\neq i}^{M} \frac{(\mu_m^i(t)-\mu_m^j(t))}{d_{ij}^2(\mu_m^i(t),\mu_m^j(t))-\alpha^2}],$$
$$\Rightarrow \mu_m^i(t_k), i=1,\dots,N_m, \tag{36}$$

Processing of crowd data $y_c([t_k-T,t_k])$ (37)

RHO with data assimilation with sensor measurements $y_i([t_k-T,t_k])$, $i=s,m,c$:

$$\min_{z\in\Im(t),\theta\in\Theta} \int_{t_k-T}^{t_k} [\sum_{i=1}^{N_s} \frac{1}{r_s^i}\|y_s^i(\tau) - C_s^i(\mu_s^i)Z(\tau,z,u(.),\Theta)\|^2 + \sum_{i=1}^{N_m} \frac{1}{r_m^i}\|y_m^i(\tau) - C_m^i(\mu_m^i(\tau))Z(\tau,z,u(.),\Theta)\|^2$$
$$+ \sum_{i=1}^{N_c} \frac{1}{r_c^i}\|y_c^i(\tau) - C_c^i(\mu_c^i(\tau))Z(\tau,z,u(.),\Theta)\|^2\ ]\ d\tau + \|z-\hat{z}(t_k-1)\|_{M_1^{-1}}^2 + \|\theta-\hat{\theta}_{k-1}\|_{M_2^{-1}}^2, \tag{38}$$
$$\Rightarrow \hat{z}([t_k-T,t_k]), \hat{\theta}_k$$

[2] Here, constraints $d_{ij}(t) \leq \beta$ are omitted.

Repeat the above steps for all t_k, using

$$\mu_m([t_k - T, t_k]), \mu_c([t_k - T, t_k]), y_s([t_k - T, t_k]), y_m([t_k - T, t_k]), y_c([t_k - T, t_k]) \quad (39)$$

where the $1/r_i^j$, $i = s, m, c$ denote the degree of confidence in the sensor i j measurement or the quantitative data provided by crowdsensing.

Finally, Fig. 5 depicts the overall proposed scheme.

6. TWO ILLUSTRATIVE CASE STUDIES

The goal of this section is to illustrate how OSSP techniques (25), (29) and RHO approach (33) described in the previous sections, can be applied to realistic hazard monitoring problems.

The section is now dedicated to two main topics:

(1) The management of both static and mobile sensor networks in the context of air pollution monitoring.

(2) The early detection of fire ignition and the prediction of the spreading of wildfires based on a receding using low-cost temperature sensors deployed on the field. To the best of my knowledge, such a RHO has never been proposed before.

6.1 Optimal management and deployment of static or mobile Sensor networks for air pollution monitoring

This section sums up some contributions in ([Georges (2011)], [Georges (2013a)], and [Georges (2017)] and presents the following results:

- The management of a WSN with static sensor nodes including lifespan concern;
- The illustration of navigation strategy (29) with a number of UAVs reaching 100 units;
- A modal observability metric not proposed in my previous publications.

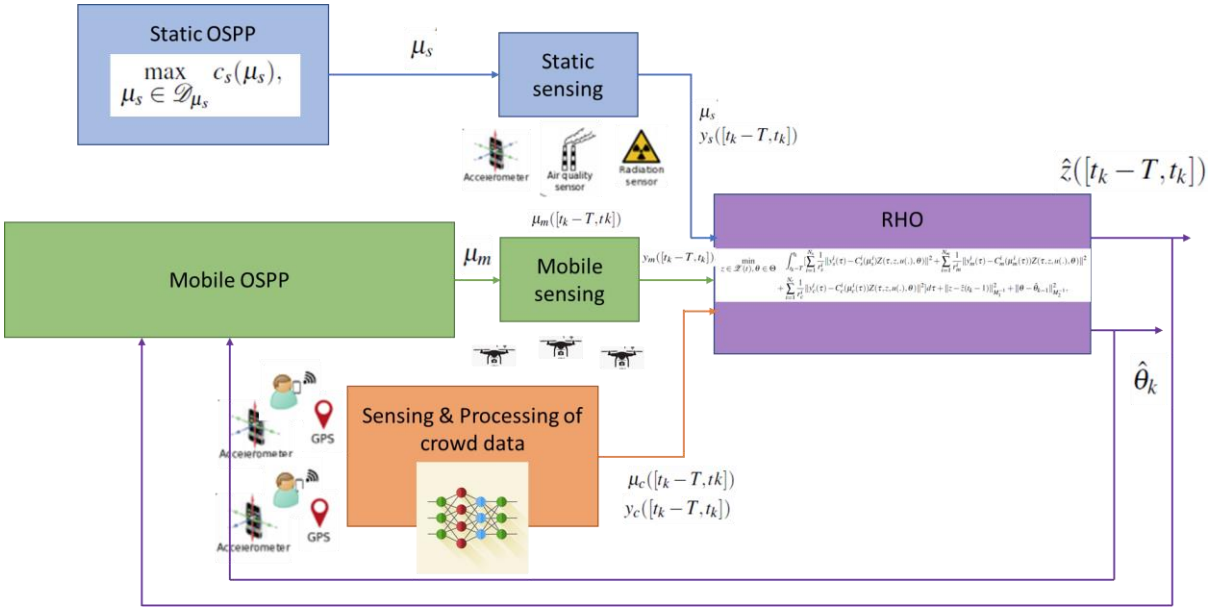

Figure 5. Optimal Monitoring Architecture.

Air pollution spreading is classically modeled by 2D or 3D advection-diffusion partial differential equations (ADPDE) (see [Zannetti (1990)] for example). For the sake of simplification, only a 2D problem is discussed here.

$$\frac{\partial z}{\partial t}(x,t) + U(x,t).\nabla z(x,t) = k\Delta z(x,t) + D(x,t)S(t) - rz(x,y,t) \tag{40}$$

where $z(x,t)$ is the concentration of a chemical species, $U = (U_x, U_y)$ is the vector of wind velocities, k is the diffusion coefficient, r is the reaction coefficient, $S(t)$ represents the source of pollution assumed to be known, $D(x,t)$ represents how the source of pollutant $S(t)$ acts in a domain $\Omega = [0,L]\ [0,H]$, where L and H are the limits of the *2D* domain. ∇ is the gradient operator, while Δ is the Laplacian operator.

Some initial conditions $z(x,u,t = 0) = z_0(x,y)$ and boundary conditions are needed for the well-posedness of the problem, for instance, Dirichlet boundary conditions:

$$z(x,y,t) = z_{bc}(x,y,t), \forall (x,y) \in \partial\Omega \tag{41}$$

In what follows, the source is supposed to be constant with a gaussian distribution located at (x_s, y_s).

Three methods will be considered in the following sections to deal with a finite-dimensional system of form (31):

- A time-explicit finite-difference approximation [Georges (2011)];
- A spectral Galerkin methods [Georges (2013a)] using Legendre's orthogonal polynomials;

- A modal approximation based on the solution of the eigenvalue problem of the advection-diffusion equation (40) ([Georges (2017)]. More focus on this appraoch will be made in section 6.1.2.

6.1.1 Managing the trade-off between observability and energy consumption in static Wireless Sensor Networks

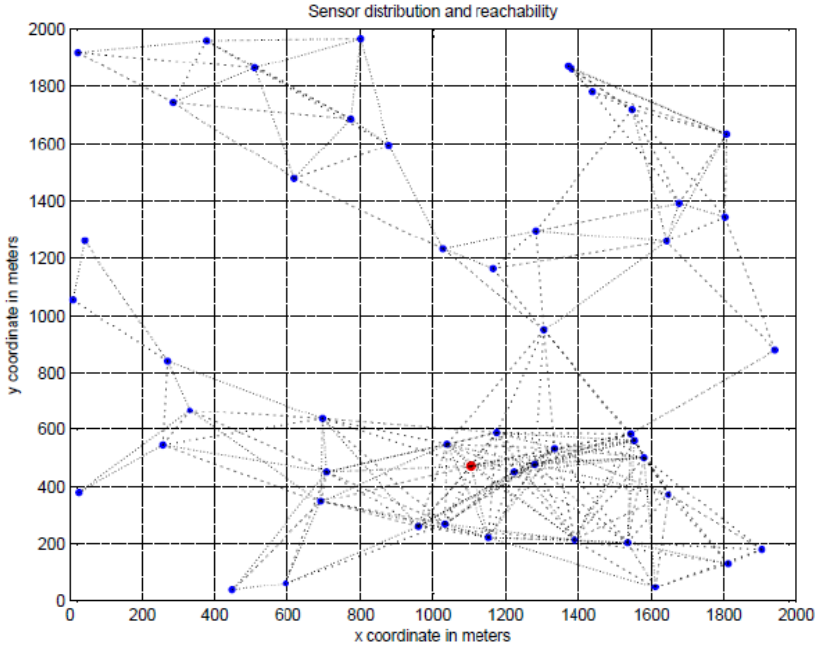

Figure 6. Static network of 50 randomly-distributed sensors with 296 communication links, on a monitored square domain of 2*km* side.
The dotted lines feature the existence of an effective communication link between two sensors (mutual reachability). The red dot is the sink station.

In [Georges (2011)], the problem of energy management in a static WSN, ensuring the best possible observability of air pollution, while maximizing the lifespan, was studied. This section sums up the contribution and the main results obtained. It can be regarded as a special case of OSPP (25) where constraints on energy and communications were taken into account.

The sensors were assumed to operate with limited energy harvesting and storage capabilities. The chosen observability metric was the trace of the observability gramian (20).

Two objectives were assigned:

- The first objective consisted in maximizing the observability index.
- The second objective was to maximize the lifespan of the network by minimizing the energy consumed by the sensors (due to communication and data processing).

It is worth noticing that these objectives are antagonistic and there is a trade-off to find, since observability is better if many sensors are active, but the price to pay is a greater energy consumption of the sensors.

The sensors were assumed to be equipped with a battery and a photovoltaic panel.

This problem was formulated in [Georges (2011)] as a two-objective optimization problem using a receding horizon optimization problem constrained by the topology of available communication links which depends on both the initial configuration of the network and the individual state of the sensors (the fact to be active in sensing or not).

The network structure is described in Fig. 6.

The incidence matrix M_I of the communication network is assumed to be known. It is derived from the connectivity matrix of the network, that depends on the interdistance d_{ij} between any sensor nodes i and j. If δ is the M_c vector of the δ^{ij}'s, where δ^{ij} denotes the average number of packets routed from the node i to the node j and $Mc = \sum_{i,j} \beta_{ij} = \sum_{i=1}^{M} card(C_i)$, where for each node i, C_i denotes the set of the nodes connected to i: $C_i = \{j, j = 1,\dots,M, j \neq i/\beta_{ij} = 1\}$, we get the following model of communications links:

$$M_I \delta + d\alpha - Hd_0 = 0_{Mc\times 1}, \tag{42}$$

where d is the maximum number of packets transmitted by any sensor node (routing information and measurement packets), d is supposed to be fixed. $H = (1,\dots,0)^T$, and d_0 is the maximum number of packets received by the base station. Since all the packets are supposed to converge towards the base station, $d_0 = \sum_{i=1}^{M} d\alpha^i$.

Decision variable $\alpha^i \in [0,1]$ was introduced to reflect the activity ratio of node i (when $\alpha_i = 1$, node i is fully active, while when $\alpha_i = 0$ it is in standby).

The amount of energy needed to send a packet of the measurement data, status and routing data between the node i and the node j is assumed to be available on request of the base station, and is given by a coefficient $k_{ij}^s > 0$. k_{ij}^s depends on the distance d_{ij} between node i and node j, since the emission power needed to send packets to node j increased as a function of the distance d_{ij}. On the other hand, the amount of energy needed to receive a packet from the node j is given by a coefficient $k_{ij}^r > 0$. The a model of energy consumption at each node i, $i = 1,\dots,M$ is given by:

$$\dot{e}^i(t) = -\boldsymbol{k_{ii}}\alpha^i(t) - \sum_{j\in C_i} [k_{ij}^s \delta^{ij}(t) + k_{ij}^r \delta^{ji}(t)] + E^i(t) - p^i(t) \tag{43}$$

$$\underline{e}^i \leq \underline{e}^i(t) \leq \overline{e}^i, \tag{44}$$

$$p^i(t) \geq 0, \tag{45}$$

where $e^i(t)$ is the available energy of node i at time t, e_I^i is the initial available energy stored in the node battery, and $E^i(t)$ is the energy provided by the solar cell of the sensor i at time t. The coefficient k_{ii} correspond to the energy consumed by the node i when it collects and computes its own air pollution measurement. $\underline{e}^i$ and $\overline{e}^i$ are the discharge and full battery bounds, respectively. $p^i(t)$ is a energy "spill" variable to take into account the full battery state.

The OSSP may be now formulated as a two-goal receding horizon control problem as follows[3]

$$\min_{\delta(t_k),\alpha(t_k),d^L(t_k),p(t_k)} \int_{t_k}^{t_k+T} \{ \sum_{i=1}^{M} (k_{ii}\alpha^i(t) + \sum_{j\in C_i} [\, k_{ij}^s(d_{ij})\delta^{ij}(t) + k_{ij}^r\delta^{ji}(t)]) + K_p \sum_{j=1}^{M} (p_l^j + d_{jl}^L) - \sigma\, trace(W(t_k, T_0, \alpha(t)))\} \tag{46}$$

subject to constraints

$$M_l M\delta(t) + d\alpha(t) - H\sum_{i=1}^{M} d\alpha^i(t) - d^L(t) = 0_{M_c\times 1}, \tag{47}$$

$$\dot{e}^i(t) = -k_{ii}\alpha^i(t) - \sum_{j\in C_i} [k_{ij}^s\delta^{ij}(t) + k_{ij}^r\delta^{ji}(t)] + \hat{E}^i(t) - p^i(t) \tag{48}$$

$$e_0^i = e_I^i, \tag{49}$$

$$\underline{e}^i \leq \underline{e}^i(t) \leq \overline{e}^i, \tag{50}$$

$$0 \leq \delta^{ij}(t) \leq \bar{\delta}^{ij}(d_{ij}), 0 \leq \alpha^i(t) \leq 1, d^L(t) \geq 0, p^i(t) \geq 0, \tag{51}$$

where $\sigma > 0$ is the "preference or arbitrage coefficient", and $K_p > 0$ is a large enough penalty coefficient, $W(t_k, T_O, \alpha(t))$ is the observability gramian of the discretized ADPDE obtained by finite-differences, computed on the time interval $[t_k - T_O, t_k]$, $\hat{E}^i(t)$ is a prediction (except at current time t) of the amount of energy provided by the solar cell (depending on both night or day time and weather conditions). $e^i(t)$ is the amount of energy stored in the battery, available for the node i at t. $\bar{\delta}^{ij}(d_{ij})$ is the maximum number of packets sent by the node i to the node j at every sampling time (a data flow rate limit), which will depends on the inverse of the distance d_{ij} since the transmission rate is affected by the quality of the wireless link. $d^L(t)$ is the M vector of packet losses at each node. Packet losses may occur, when some links are congested due to data flow rate limits.

Based on the parameters of the ADPDE, the 50-sensor network, and the optimization given in [Georges (2011)], Fig. 7a and Fig. 7b provide a comparison of the results obtained with two different values of preference coefficient σ, 2 and 0.1. The trade-off is in favour of the observability maximization when the value of σ is large (see the left column results compared

[3] In the referenced paper, the formulation was originally made in discrete-time.

to the right column results with the smaller value of σ). All the results are expressed in normalized units. The different figures show the evolution on 24 hours of the observability index, the evolution of the energy stored in each sensor, and the communication traffic in each active links of the sensor network. Not surprisingly, the observability index reaches its maximum value when a maximum of energy is available in the sensor batteries as expected. For σ = 2, the observability index value appears to be 5 times greater than when using σ = 0.1. Of course, the price to pay is a higher energy consumption of the sensors.

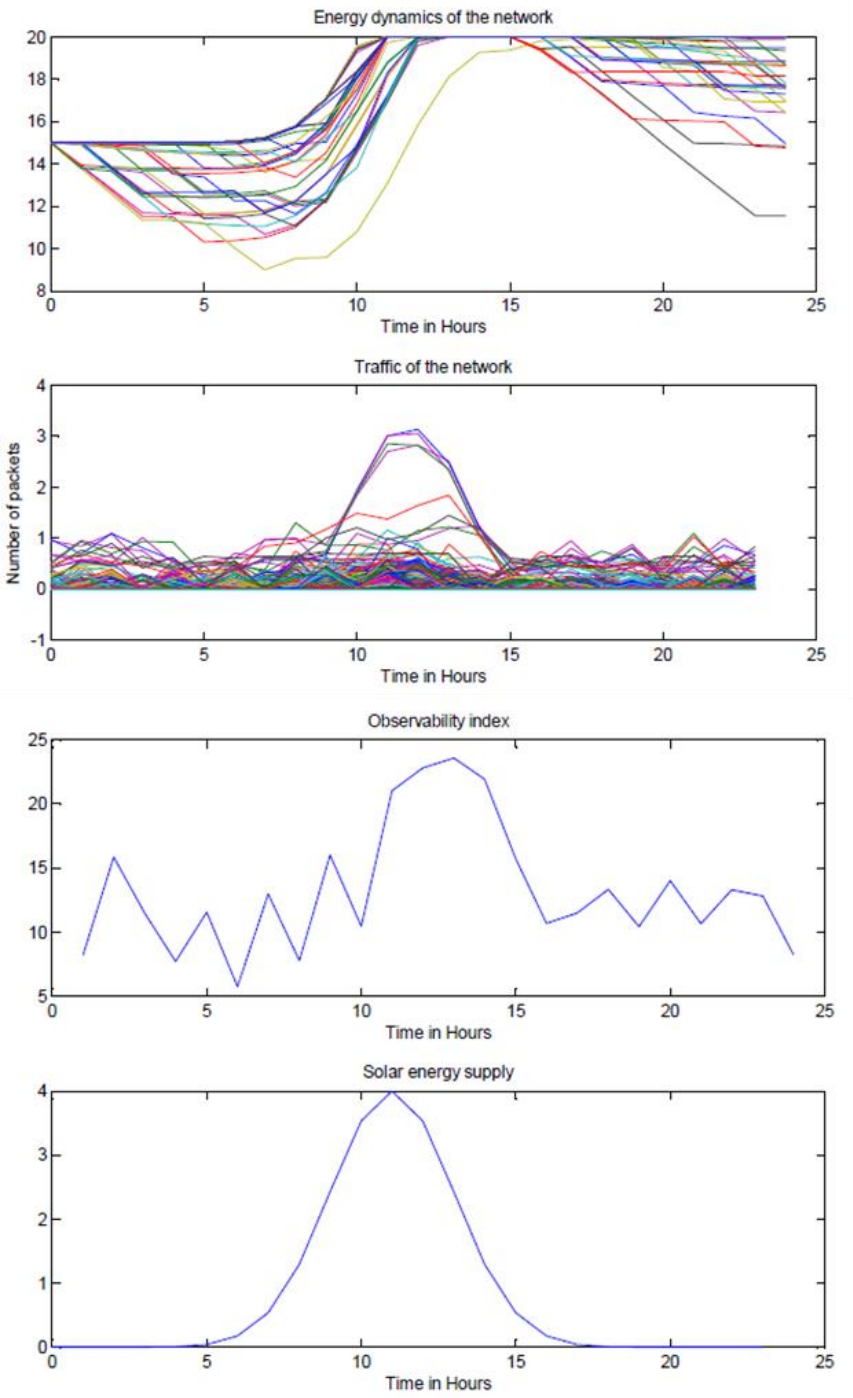

Figure 7a. Results obtained with σ = 2.,

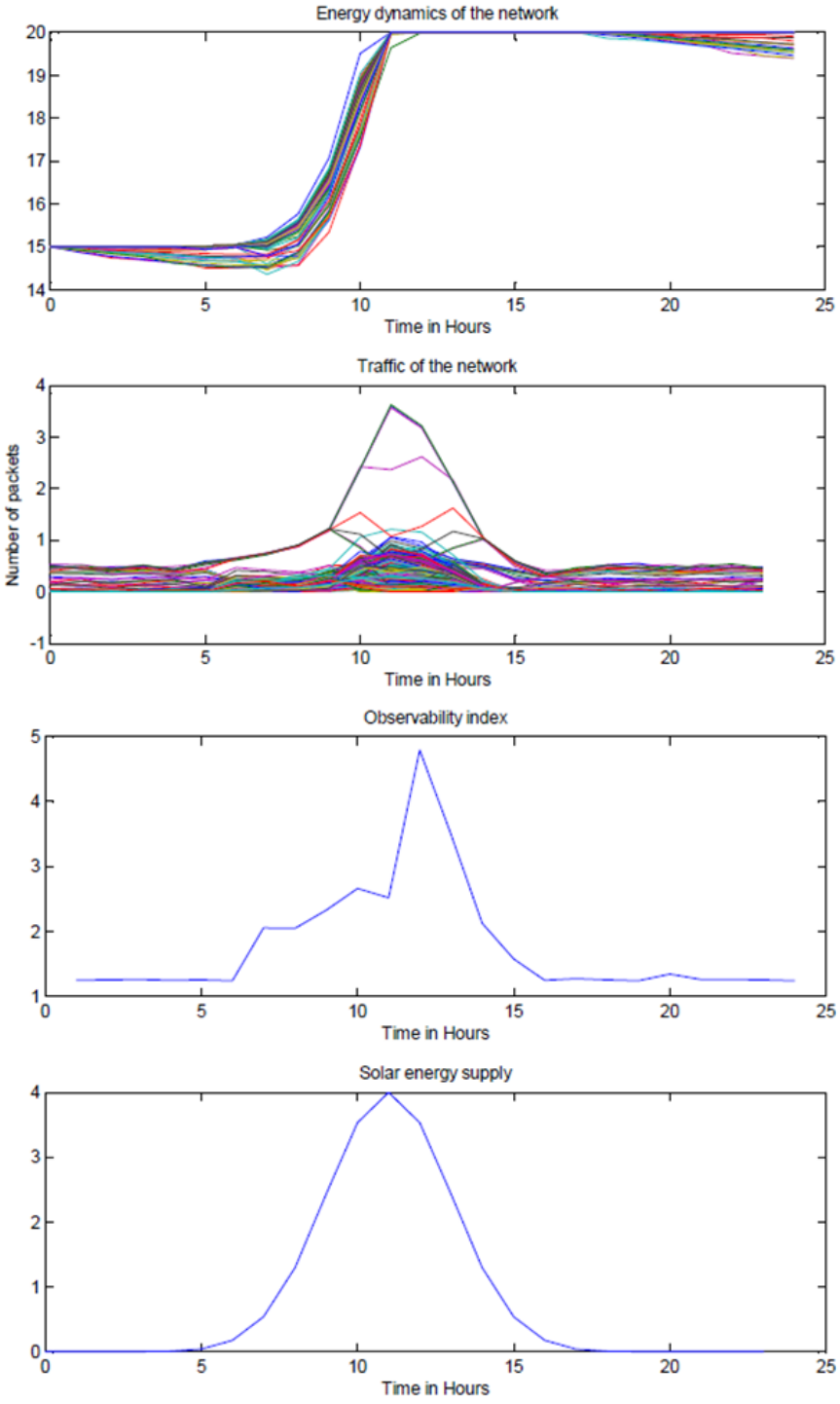

Figure 7b. Results obtained with σ = 0.1.

6.1.2 Management of mobile sensors for air pollution monitoring

This section sums up the contribution in [Georges (2013a)], where the goal was to manage mobile sensors to ensure the best possible observability of air pollution when the meteorological conditions (essentially, the wind velocity field) vary. A group of mobile sensors (UAVs) was coordinated to adapt their positioning in order to always maximize the trace of the observability gramian, while maintaining wireless communication through the group, together with mutual obstacle avoidance.

20 mobile sensors follow navigation strategy (29) that consisted in maximizing the trace of the observability gramian (20) of a reduced model of ADPDE obtained with a spectral Galerkin method using 20 Legendre's orthogonal polynomials. The individual trajectory of each sensor towards an optimal sensor configuration was constrained to guarantee mutual collision avoidance and to maintain the communication connectivity with all the other members of the group.

Table 3 shows the parameters retained for the case study presented here-after.

Table 3. ADPDE parameters

U_x	U_y	diffusion k	B.C.	D(x,t)
10km/h	10km/h	1	$z_{bc}(x,t)$ =0	$e\frac{-\|x-x_s\|^2}{2\sigma^2}, \sigma = 0.01$

The source of pollutant was assumed to be defined by a Gaussian distribution, where x_s is the source location here situated at the center of the square domain.

Fig. 8 and 9 show the trajectories of the 50 sensors to reach optimal location maximizing the observability index. The sensors start from a random initial position. On Fig. 9, the wind velocity has changed (from (10km/h, 10km/h) to ($-$ 10km/h, 5km/h)) and the sensors automatically reposition themselves to maximize the observability index corresponding to this new situation.

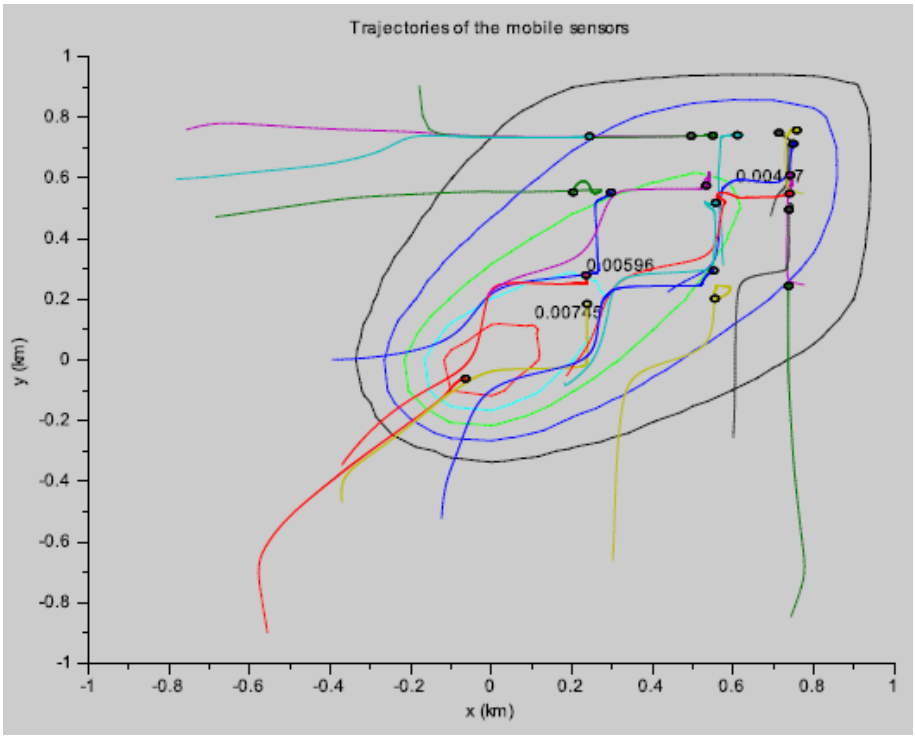

Figure 8. The ”o”’s feature the optimal location of the sensors.
The coloured curves represent levels with identical polllutant densities.

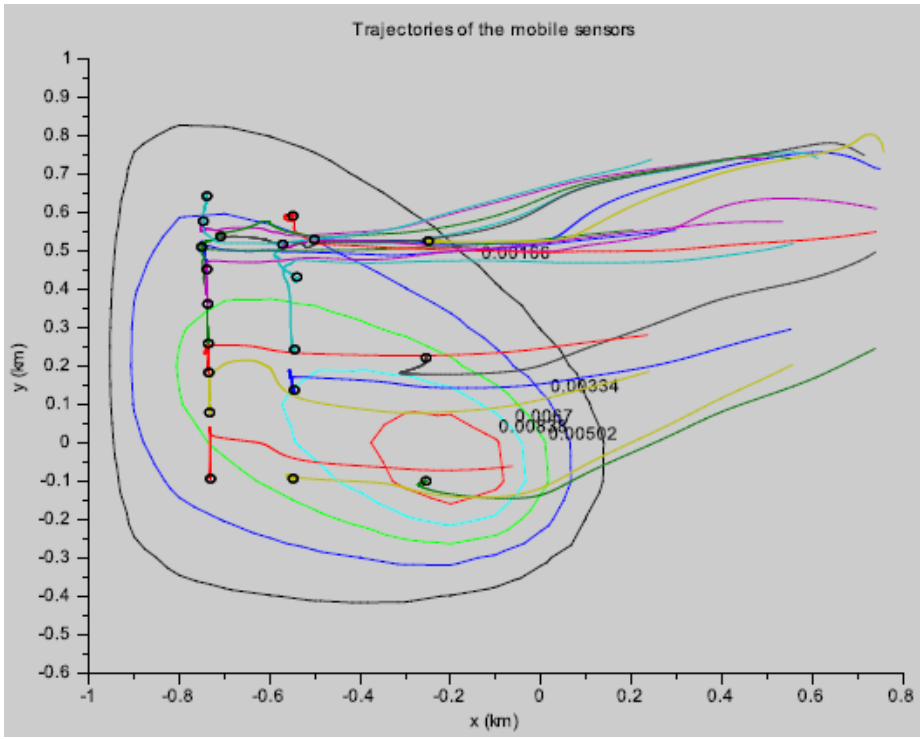

Figure 9. New trajectories of the sensors obtained after wind velocity changes.

6.1.3 OSPP with a modal observability gramian

Following [Georges (2017)], the air pollution model (40) may be represented in abstract form by

$$\dot{z}(t) = Az(t), \tag{52}$$

$$y(t) = Cz(t), \tag{53}$$

where A is the infinitesimal generator of a C_0-semigroup $T(t)$ on a Hilbert space Z, and C is an output linear and bounded operator from Z to a Hilbert space Y; define for some finite $T_o > 0$, the observability map of (A,C) on $[0,T_o]$, as the bounded linear map $C^{T_o}: Z \rightarrow L_2([0,T_o];Y)$ given by $C^{T_o}z = CT(.)z$.

Here the output operator C is given, as in (34), by

$$y = Cz = \int_0^L \int_0^H \Delta(x - x_l, y - y_l) z(x,y,t) dx dy, \tag{54}$$

where $\Delta(x - x_l, y - y_l)$ is a shaping function of a sensor l located at position $\mu_l = (x_l, y_l)$.

Here

$$\Delta(x - x_l, y - y_l) \begin{cases} 1, if(x,y) \in [\mu_l - \varepsilon, \mu_l + \varepsilon], \\ 0, otherwise. \end{cases} \tag{55}$$

The observability gramian of (A,C) is defined by the linear self-adjoint operator $W^T = C^{T_{0*}} C^{T_0}$.

In order to get an explicit form of the gramian, the following procedure was proposed in [Georges (2017)]:

(1) Transform the ADPDE (40) into the following diffusion equation:

$$\frac{\partial v}{\partial t}(x,y,t) = k \frac{\partial^2 v}{\partial_{x^2}}(x,y,t) + k \frac{\partial^2 v}{\partial_{y^2}}(x,y,t) + S'(x,y,t) - qv(x,y,t), \tag{56}$$

with $q = r + \frac{1}{4}(\frac{v_x^2}{k} + \frac{v_y^2}{k})$, thanks to the change of coordinates $z(x,y,t) = v(x,y,t)e^{p_1 x + p_2 y}$ where $p_1 = \frac{v_x}{2k}, p_2 = \frac{v_y}{2k}$.

(2) Compute the well-known eigenvalues and eigenfunctions of the diffusion equation using Dirichlet's boundary conditions:

$$\mu_n = \frac{\pi^2 n^2}{L^2}, \phi_x^n(x) = sin(\frac{n\pi x}{L}), \tag{57}$$

$$\mathrm{v}_m = \frac{\pi^2 m^2}{H^2}, \phi_y^m(y) = sin(\frac{m\pi y}{H}), \tag{58}$$

$$\phi_{nm}(x,y) = \phi_x^n(x) \times \phi_y^m(y). \tag{59}$$

(3) Get the modal solution of ADPDE (40) with input $S(x,y,t) = 0, \forall t \geq 0$:

$$z(x,y,t) = \sum_{n=1}^{\infty} \sum_{m=1}^{\infty} c_{nm} e^{(-q-k(\mu_n+v_m))t+p_1x+p_2y} \phi_{nm}(x,y), \tag{60}$$

where c_{nm} denote the modal coordinates of the initial conditions.

(4) Compute the output map using (54):

$$C^{T_0} z = \sum_{n,m=1}^{\infty} c_{nm} C_{nm}(\mu_l) \times e^{(-q-k(\mu_n+v_m))t},$$

where

$$C_{nm}(\mu_l) = \int_0^L \int_0^L \Delta(x-x_l, y-y_l) \sin(\frac{n\pi x}{L}) \sin(\frac{m\pi x}{H}) e^{p_1x+p_2y}\, dxdy \neq 0, \forall n,m, \tag{61}$$

$$\times \sin(\frac{m\pi x}{H}) e^{p_1x+p_2y}\, dxdy \neq 0, \forall n,m, \tag{61}$$

Since

$$W^{\infty}(\mu) = \sum_{n=1}^{N} \sum_{m=1}^{M} \frac{C_{nm}^2(\mu)}{2\left(k\left(\mu_n + v_m\right) + q\right)}, \tag{62}$$

where (*M*,*N*) are the numbers of modes retained for the approximation.

Fig. 10 shows the value of the observability index for a pollution distribution with constant wind velocities according to the sensor location in the domain.

Fig. 11 shows the mobile OSPP of a network of 100 mobile sensors using navigation strategy (29) with the cost function $c\left(\mu_1, \ldots \mu_{100}\right) = \sum_{i=1}^{100} trace\ \{W^{\infty}(\mu_1)\}$ on a given time period.

According to the classical theory of Riesz-spectral operators, ADPDE (40) is approximately observable if and only if all the $C_{nm}(\mu)$ are different from zero, for a sensor located at μ (see [Curtain et al (1995)]).

Then an observability index ensuring approximate observability on the basis of the first (*N*,*M*) modes can be defined by

$$c(\mu) = \min_{n=1,\ldots,N, m=1,\ldots,M} |C_{nm}(\mu)|. \tag{63}$$

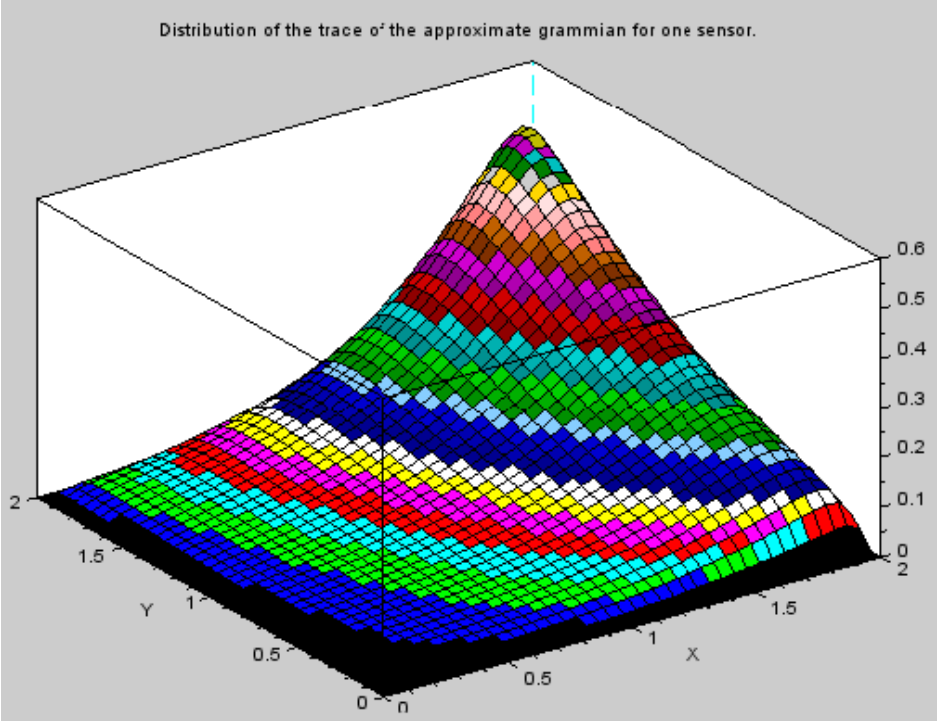

Figure 10. Observability index given by the trace of the observability gramian with $N = M = 20$ for one sensor according to its location in the domain, for ($U_x = 50km/h$, $U_y = 25km/h$).

Fig. 12 shows all the values of this new index and therefore the locations of sensors ensuring observability ($c(\mu_l) \neq 0$), with $N = M = 30$. The maximum values of the index are obtained at the top-right corner of the domain. Compared to Fig. 10, it immediately appears that metric (63) is more demanding than (62). With (63), navigation strategy (29) is no more directly applicable since the index is not smooth. It should be modified to ensure that some optimal locations of the N_s sensors μ_l^*, l=1,...,N_s, solutions of a static nonsmooth OSPP, for instance:

$$\max_{\mu_l \in D_\mu(\mu_1,\ldots,\mu_{N_s}),l=1,\ldots,N_s} \min_{n=1,\ldots,N,m=1,\ldots,M} \sum_{k=1}^{N_s} |\, C_{nm}(\mu_k)|, \tag{64}$$

are reached, for instance, by replacing the gradient $\nabla_{\mu_i} c$ by $-\gamma\,(\,\mu_i^* - \mu_i\,)$, γ >0 in (29). $D_\mu(\mu_1, \ldots, \mu_{N_s})$ is the set of constraints intended to avoid sensor clustering and to ensure inter communications between the sensors.

6.2 Early detection of a wildfire ignition and fire prediction using a receding horizon observer

In this section, some new results on the use of a receding horizon observer RHO (33) are presented, based on the adjoint method proposed in [Georges (2019)]. The objective is to be

able to detect and locate early fire ignition using a sensor network constituted with ground-layer temperature sensors (see Fig. 13).

The model of a wildfire propagation can be well described by 2D coupled partial differential equations, which define the energy balance and fuel reaction rate for a wildfire in a ground layer of some given finite small thickness, on a rectangular domain $D = [0,L_x]\times [0,L_y]$ (see [Mandel *et al* (2008)]):

$$\partial_t T = \partial_x(k\partial_x T) + \partial_y(k\partial_y T) - v_x\partial_x T - v_y\partial_y T + A(Sr(T) - C(T-T_a)), \quad (65)$$
$$\partial_t S = -C_S Sr(T),$$

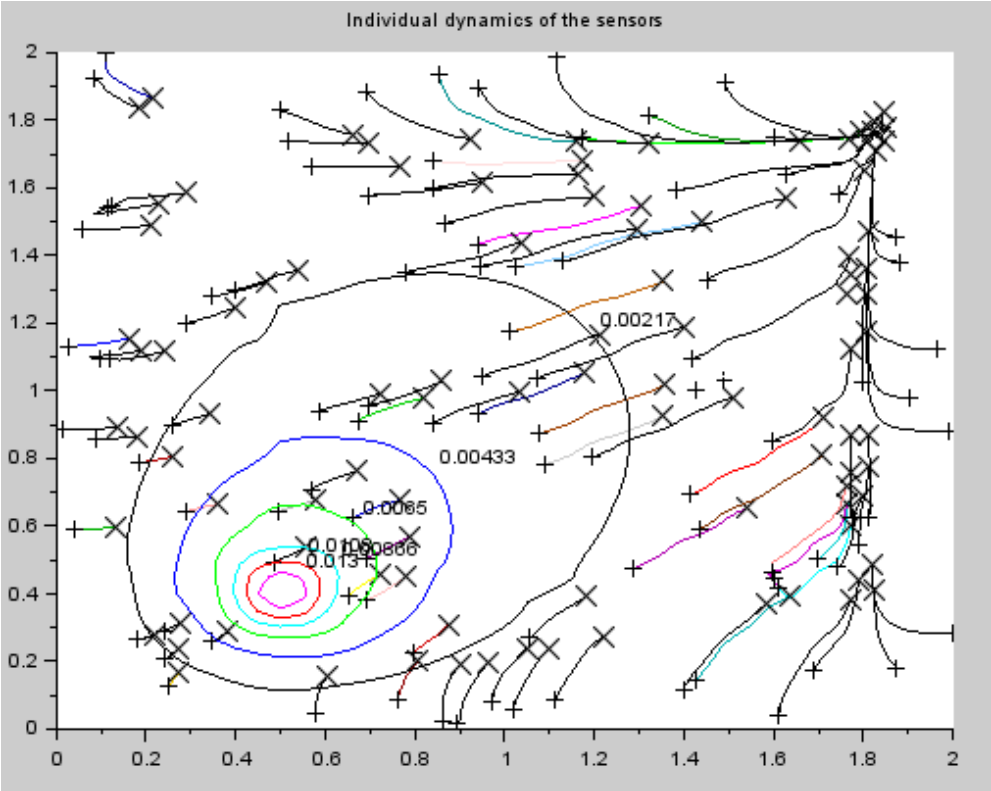

Figure 11. The 100 sensors tend to move towards locations on the right side of the domain. The sensors initially are randomly distributed in the domain. The initial locations are marked by "+", and the final ones, by "X".

with Arrhenius reaction rate from physical chemistry

$$r(T) = \begin{cases} e^{-B/(T-T_a)}, & T > T_a, \\ 0, & T \leq T_a, \end{cases} \quad (66)$$

and where $T(x,y,t)$ is the distributed temperature in the ground layer, $S(x,y,t)$ is the distributed mass fraction of fuel. k is the coefficient of temperature diffusion. $v = (v_x(x,y,t), v_y(x,y,t))$ defines the velocity field of the air, supposed to known from meteorological data. A, B, C, C_s are some

physical coefficients. T_a is the ambient temperature. ∂_t , ∂_x , and ∂_y denote the partial derivatives with respect to time *t*, and spatial coordinates *x* and *y*, respectively.

Some boundary and initial conditions have also to be defined to ensure the well-posedness of the problem. Neumann's boundary conditions are used in this paper:

$$\partial_x T(0,y,t) = \partial_x T(L_x,y,t) = 0, \forall y \in [0,L_y], \quad (67)$$

$$\partial_y T(x,0,t) = \partial_y T(x,L_y,t) = 0, \forall x \in [0,L_x], \quad (68)$$

$$T(x,y,0) = T_0(x,y), S(x,y,0) = S_0(x,y), \forall (x,y) \in D. \quad (69)$$

The interest of this model relies in the fact it is able to simulate heat travelling waves in a realistic way. In what follows, a normalized model is adopted (see (71) and (72)).

A network of temperature sensors is assumed to be deployed in the field. The location of the sensors is obtained thanks to a Sobol's sequence (see [Georges (2019)]. The sensor location is assumed to be fixed and the effect of changes in wind direction is taken into account via the advection term of model (65) by using weather forecast data. A perspective would be to use mobile sensors (UAVs with infrared sensors) using a navigation strategy (26) or (29). Here it is assumed that the initial fuel distribution *S*(*x*,*y*,0) is known from an a priori mapping of the field. Physical coefficients β and λ are also assumed to be known from the knowledge of previous wildfire occurrences with the same fuel characteristics.

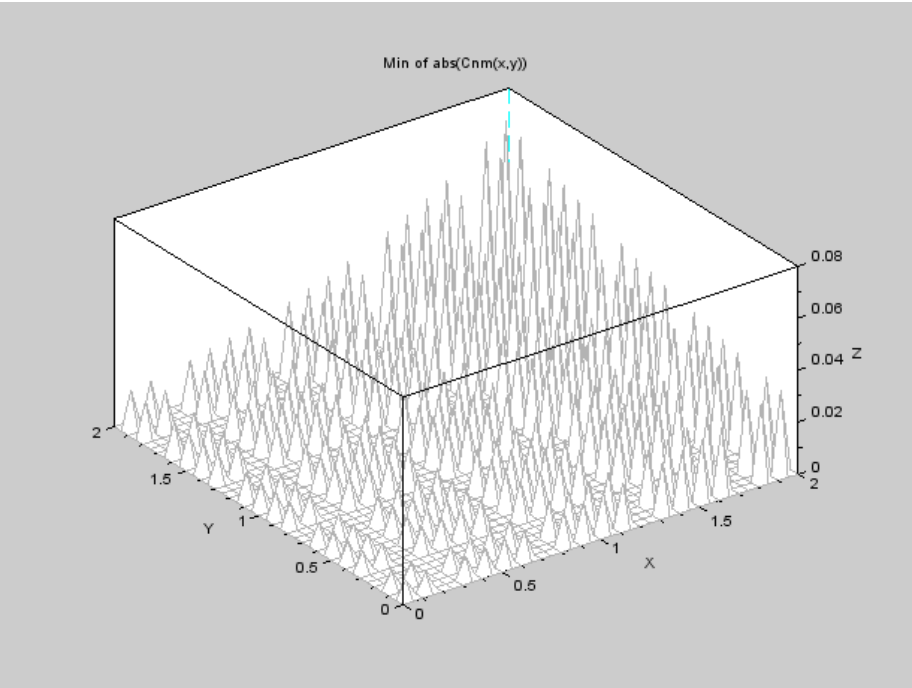

Figure 12. Alternative modal observability index over the domain. Observability for $N = M = 20$ is ensured only on very specific locations.

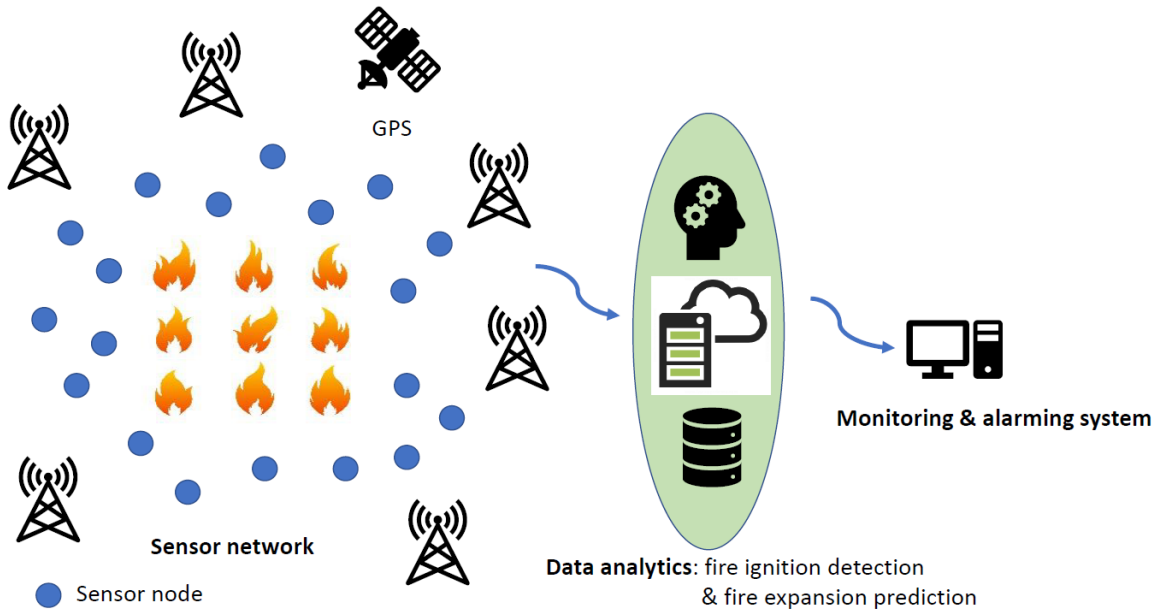

Figure 13. Sensor networks for wildfire monitoring (see also [Li *et al* (2006)]).

Similarly to (33), the moving horizon fire ignition estimation will consist in finding the distributed temperature at each time instant t_k over domain D. This can be formulated as solving the optimal least-square optimization problem defined for N_s sensors and on moving time interval $[t_k - T_f, t_k]$:

$$\min_{T(x,y,t_k-T_f)\in D} J(T_0) = \min_{T(x,y,t_k-T_f)\in D} \frac{1}{2}\sum_{i=1}^{N_s} \int_{t_k-T_f}^{t_k} (y_i(t) - y_i^m(t))^2 dt + \frac{a}{2}\int_0^{L_x}\int_0^{L_y} (T(x,y,t_k-T_f))^2 dxdy, \quad (70)$$

subject to

$$\partial_t T = \partial_{xx} T + \partial_{yy} T - v_x \partial_x T - v_y \partial_y T + Se^{-1/T} - \lambda T, \quad (71)$$

$$\partial_t S = -\beta S e^{-1/T}, T > 0, \quad (72)$$

where the measurement operator for each sensor i is given by

$$y_i(t) = \int_0^{L_x}\int_0^{L_y} \Delta(x - x_s^i, y - y_s^i) T(x,y,t) dxdy, \quad (73)$$

Where $y_i^m(t)$ is the temperature measured by sensor i at time t and pair $\mu_i = (x_s^i, y_s^i)$ denotes the spatial coordinates of sensor i in the reference frame. Δ is defined as (55). This problem was solved by using a adjoint-based method associated to a gradient iterative algorithm. The PDEs are discretized using a finite difference scheme on a 80×80 grid leading to a finite-dimensional system of 6400 states. The interested reader may refer to [Georges (2019)] for the derivation of the necessary conditions for optimality and the detailed computation of a closely-related state estimation problem without receding horizon technique.

In the simulation presented here-after, the receding horizon is equal to 160 time samples, and the domain is assumed to be a square of size 650 (in normalized units) for each side. The fuel is uniformly distributed over the domain, except for a fuel break featuring a river with no fuel. The fire ignition is detected when at least a sensor measures an abnormal temperature increase implying that the cost function of (70) becomes greater than a small threshold. The detection time is not the fire ignition time, since the fire wave reaches the closest sensor after a propagation time delay. Fig. 14 shows the fuel consumption after 160 time samples. The fire ignition was located at (450,350) and modelled by a gaussian distribution. Fig. 15 shows the location over the domain of the 50 temperature sensors used by the RHO algorithm (meaning that only 0.8% of the 6400 system states are supposed to be known). Fig. 16 shows a comparison between the estimated distribution of the fire ignition and the simulated one. Finally, Fig. 17 demonstrates that the RHO is able to predict the wildfire expansion, despite the fact that the data assimilation problem is known to be ill-conditioned. The optimization problem appears to be very sensitive to initial conditions that are generated randomly. Several trials (here 5) have to be performed at each sample time t_k and the solution corresponding to the minimum value of the cost function is retained.

7. CONCLUSIONS AND PERSPECTIVES

This paper was devoted to the design of optimal architectures for hazard assessment monitoring. Hazard assessment monitoring was viewed as the ability of estimating and predicting states of a dynamical system representing a natural or technological hazard. It was also considered to be the ability to estimate model parameters or changes in the model parameters. From the view point of risk assessment, the proposed approach can be used to detect vulnerabilities or locate failures or dysfonctionning, and to predict future behaviors of the hazard in time or space. In this paper, two approaches were discussed: firstly, the key notion of system observability was emphasized and some metrics for measuring observability were discussed. The use of these metrics was also investigated for solving the optimal sensor location problem for both static or mobile sensor networks. A survey of applications of such optimal sensor location problem was also provided. Secondly, the receding horizon estimation approach was presented. The relevance of this estimation technique was discussed and a survey of existing and potential applications of this approach was also proposed. Finally, some concrete applications illustrating optimal sensor location problems and receding horizon estimation were presented in the field of air pollution and wildfire monitoring.

The application of the framework described in this paper to large-scale cascading hazards is still a big challenge to be investigated. In that context, one key issue is the availability of effective model reduction techniques suitable for large-scale complex dynamics of coupled phenomena. Furthermore, the implementation and validation of the global architecture (OSPP and RHO together) remain to be studied in real situations.

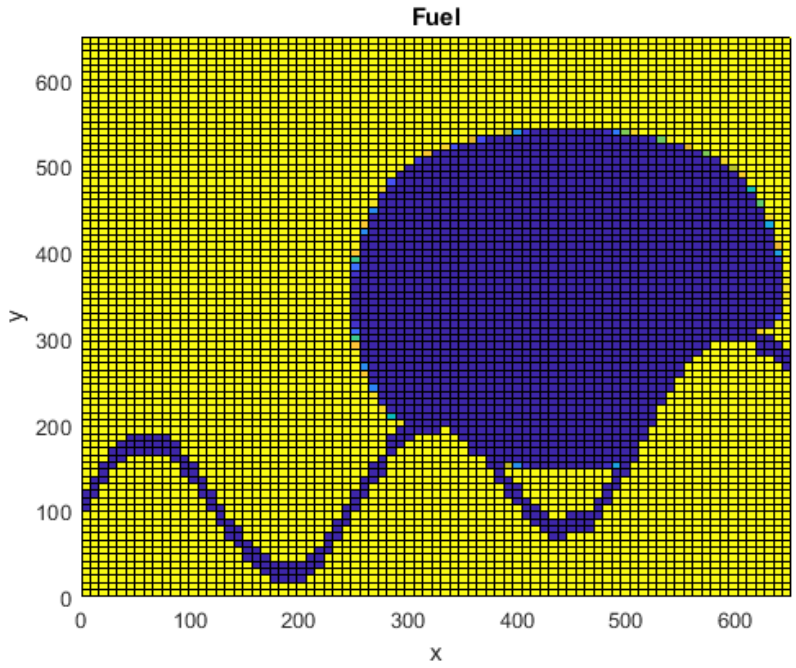

Figure 14. The burned area and the river are in blue color. The fuel consumption is given after 160 time samples.

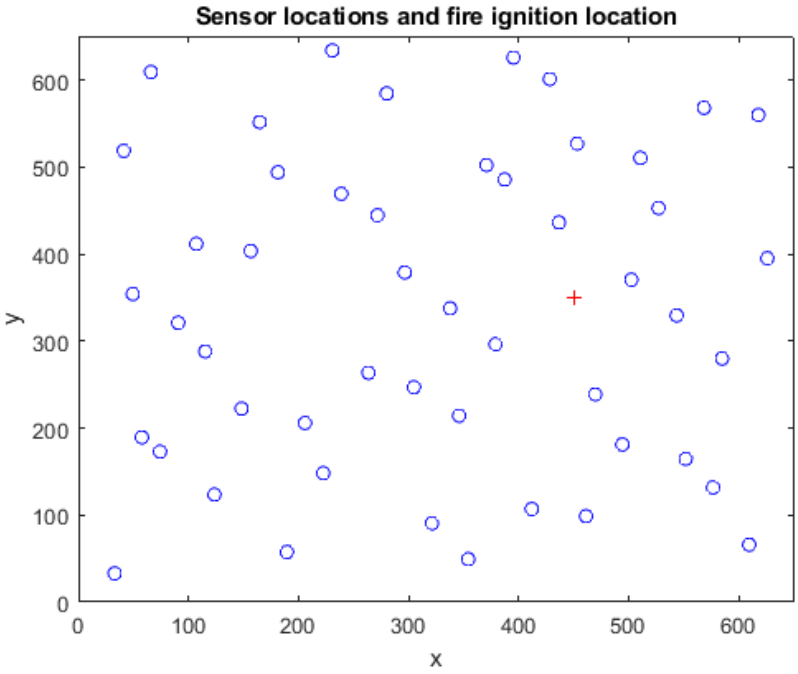

Figure 15. 50-Sensor location based on Sobol's sequence. The red "+" represents le location of the fire ignition.

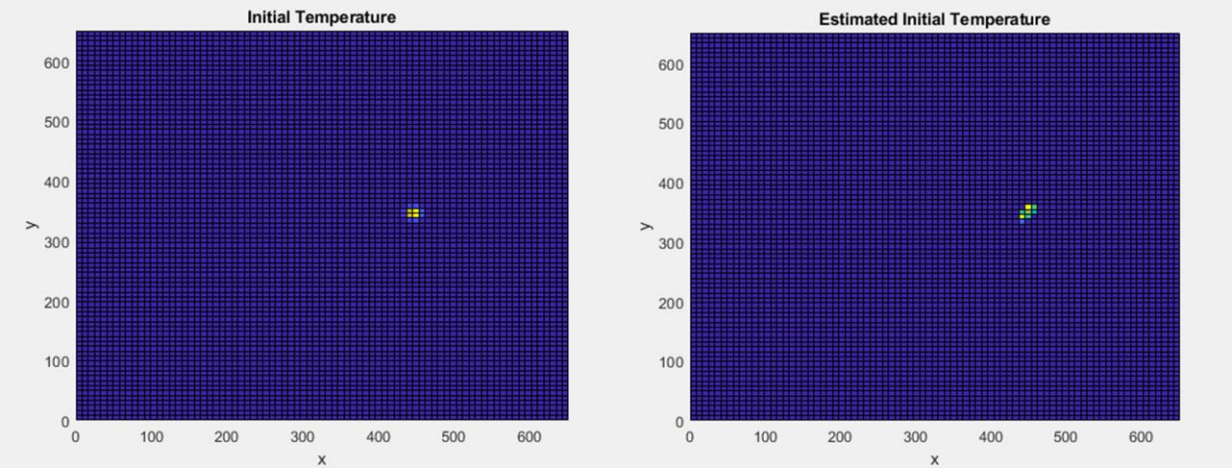

Figure 16. Comparison - Fire ignition.

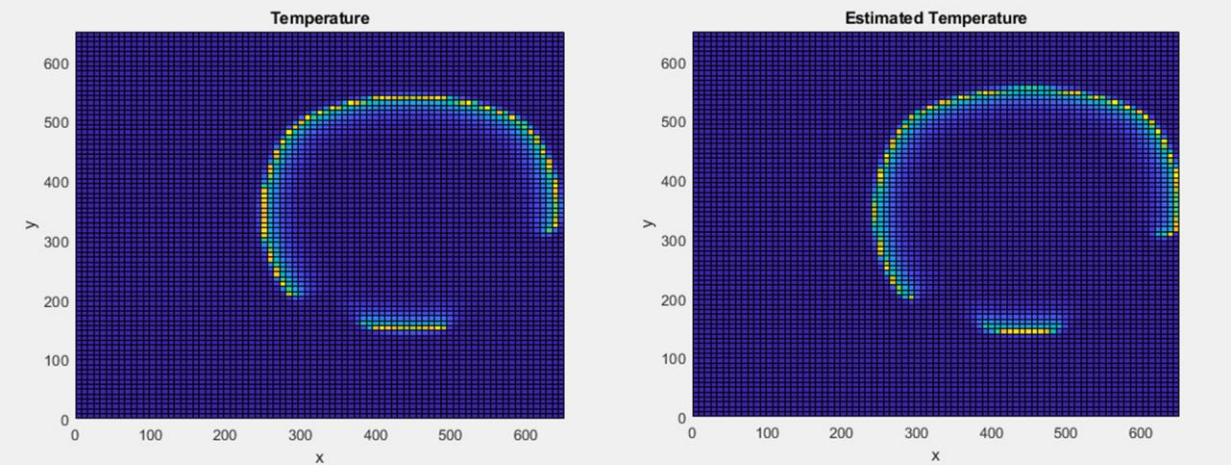

Figure 17. Comparison - Temperature distribution after t = 160 time samples.

The huge development of Internet of Things and machine learning techniques for processing data obtained by crowdsensing in the context of more and more powerful networking capabilities (5G technology) offers very large perspectives for the development of more and more accurate risk monitoring.

Such methods cannot be designed without a strong cross-disciplinary approach for including knowledge of fields, models, for qualification and preprocessing of available data, and finally developing adequate monitoring algorithms.

REFERENCES

ALAMIR, M. and CORRIOU, J.P. (2003) Nonlinear receding-horizon state estimation for dispersive adsorption columns with nonlinear isotherm, *Journal of process control*, 13 (6):517–523, 2003.

ALAMIR, M. (2007) *Nonlinear Moving Horizon Observers: Theory & Real-Time Implementation. In Nonlinear Observers and Applications, Gildas Besan¸con (Ed)*. Lecture Notes on Communication and Information Science. Springer-Verlag-Series 2007.

ALONSO, L., BARBARAN, J., CHENA, J., DIAZ, M., LLOPIS, L. and RUBIO, B. (2018) Middleware and communication technologies for structural health monitoring of critical infrastructures: A survey, *Computer Standards & Interfaces* Volume 56, February 2018, Pages 83-100.

ANTOULAS, A.C., SORENSEN, D.C. and GUGERCIN, S. (2006) A survey of model reduction methods for large-scale systems, https://www.math.vt.edu/people/gugercin/papers/survey.pdf, 2006.27

BENNER, P., COHEN, A., OHLBERGER, M. and WILLCOX, K. (2017) *Model Reduction and Approximation: Theory and Algorithms*, SIAM, 2017.

BERTSEKAS, D. P. (2015), *Convex Optimization Algorithms*, Belmont, MA.: Athena Scientific. ISBN 978-1-886529-28-1.

BESANCON, G. (Ed.) (2007) *Nonlinear Observers and Applications, Lecture Notes on Communication and Information Science*. Springer-Verlag-Series 2007.

BURER, S. and LETCHFORD, A. N. (2012) Non-convex mixed-integer nonlinear programming: A survey, *Surveys in Operations Research and Management Science* 17 (2012) 97–106.

BOSSU, R., *et al* (2018) LastQuake: From rapid information to global seismic risk reduction, International Journal of Disaster Risk Reduction, Volume 28, June 2018, Pages 32-42.

BOUBRIMA, A., MATIGOT, F., BECHKIT, W., RIVANO, H. and RUAS A. (2015) Optimal Deployment of Wireless Sensor Networks for Air Pollution Monitoring. ICCCN 2015 - 24th International Conference on Computer Communication and Networks, Aug 2015, Las Vegas, United States, hal-01171765.

CAPPONI, A., FIANDRINO, C., KANTARCI, B., FOSCHINI, L., KLAZOVICH, D., and BOUVRY, P. (2019), A Survey on Mobile Crowdsensing Systems: Challenges, Solutions and Opportunities, *IEEE COMMUNICATIONS SURVEYS & TUTORIALS*, DOI 10.1109/COMST.2019.2914030.

CASILLAS, M. V., GARZA-CASTANON, L. E. and PUIG, V. (2015) Optimal Sensor Placement for Leak Location in Water Distribution Networks using Evolutionary Algorithms, *Water* 2015, 7(11), 6496-6515; https://doi.org/10.3390/w7116496.

CURTAIN, R. F. and ZWART, H. J. (1995) *An Introduction to Infinite-Dimensional Linear Systems Theory*. Springer- Verlag, ISBN 0-387-94475-3.

DEMETRIOU, M. A., (2008) Distributed parameter methods for moving sensor networks in unison, 2008 American Control Conference Westin Seattle Hotel, Seattle, Washington, USA June 11-13, 2008.

DEMETRIOU, M. A., (2010) Guidance of mobile actuator-plus-sensor networks for improved control and estimation of distributed parameter systems, *IEEE Transactions on Automatic Control*, Vol. 55, 7, 1570-1584, 2010.

DEMETRIOU, M. A. and ARMAOU, A. (2014) Frequency domain methods for optimal sensor placement and scheduling of spatially distributed systems arising in environmental and meteorological applications, 2014 American Control Conference (ACC) June 4-6, 2014. Portland, Oregon, USA.

FERRARI-TRECATE, G., MIGNONE, D. and MORARI. M., (2003) Moving-horizon estimation for hybrid systems, *IEEE Transactions on Automatic Control*, vol. 47, no. 10, pp. 1663–1676, 2003.

GEORGES, D. (1995) The use of observability and controllability gramians or functions for optimal sensor and actuator location in finitedimensional systems. 34th IEEE Conference on Decision and Control (CDC'95), december 1995, New Orleans, (USA).

GEORGES, D. (2011) Energy Minimization and Observability Maximization in Multi-Hop Wireless Sensor Networks, 18th IFAC World Congress 2011, Milano, Italy, 2011.

GEORGES, D. (2013a) Optimal Location of Mobile Sensors for Environmental Monitoring, 2013 - 12th biannual European Control Conference (ECC 2013), Switzerland (2013) [hal-00834642 - version 1].

GEORGES, D. (2013b) Optimal Location of a Mobile Sensor Continuum for Environmental Monitoring, First IFAC Workshop on Control of Systems Governed by Partial Differential Equations (CPDE 2013), Paris, France (2013) [hal-00834645 - version 1].

GEORGES, D. (2014) Optimal PMU-based monitoring architecture design for power systems, *Control Engineering Practice*, (2014), 150- 159, http://dx.doi.org/10.1016/j.conengprac.2013.11.019.

GEORGES, D. (2017) Optimal sensor location and mobile sensor crowd modeling for environmental monitoring, IFAC 2017 World Congress, Toulouse, France, 9-14 July, 2017.

GEORGES, D. (2019) A Variational Calculus Approach toWildfire Monitoring Using a Low-Discrepancy Sequence-Based Deployment of Sensors, 2019 IEEE 58th Conference on Decision and Control (CDC), Nice, France, 2019, pp. 5912-5917, doi: 10.1109/CDC40024.2019.9029962.

GOULD, N., ORBAN, D. and TOINT, Ph. (2005) Numerical methods for large-scale nonlinear optimization, Acta Numerica (2005), pp. 299–361, *Cambridge University Press*, 2005.

HERZOG, R., RIEDEL, I. and UCINSKI, D. (2017) Optimal Sensor Placement for joint parameter and state estimation problems in large-scale dynamical systems with applications to thermo-mechanics, On-line Internal Report,Technische Universitat Chemnitz, 2017.

JOHANSEN, T. A., SUI, D. and NYBO. R. (2013) Regularized Nonlinear Moving-Horizon Observer with Robustness to Delayed and Lost Data, *IEEE Transactions on Control System Technology*, Vol. 21, No. 6, November 2013.

KAILATH, Th. (1980), *Linear Systems*, *Pientice-Hall Informations and System Sciences Series*, 1980.

KANG, W. and XU, L. (2011) Optimal Sensor Placement for Data Assimilations, https://gmao.gsfc.nasa.gov/events/adjoint workshop- 9/presentations/Xu.pdf, 2011.

KARMITSA, N. (2016) *Numerical Methods for Large-Scale Nonsmooth Optimization, in Big Data Optimization: Recent Developments and Challenges*, Springer, 2016.

KHORSHIDI, M. S., NIKOO, M. R. and SADEGH, M. (2018) Optimal and objective placement of sensors in water distribution systems using information theory, *Water Research*, Volume 143, 15 October 2018, Pages 218-228.

KING, S., KANG, W., and XU, L. (2014) Computational Issues on Observability and Optimal Sensor Locations, 2014 American Control Conference (ACC) June 4-6, 2014. Portland, Oregon, USA.

KOUICHI, H., TURBELIN, G., NGAE, P., FEIZ, A. A., BARBOSA, E., *et al* (2016) Optimization of sensor networks for the estimation of atmospheric pollutants sources, WIT Transactions on Ecology and the Environment, *WIT Press*, 2016, Air Pollution XXIV, 207, pp.11-21. ff10.2495/AIR160021ff. hal-01593828.28

KHUL, P., DIEHL, M., KRAUS, T., SCHLODER, J. P., BOCK, H. G., (2011) A real-time algorithm for moving horizon state and parameter estimation, *Computers & Chemical Engineering* Volume 35, Issue 1, 10 January 2011, Pages 71-83.

LALL S., MARSDEN, J. E. and GLAVASI, S. (1999) Empirical model reduction of controlled nonlinear systems, *IFAC Proceedings Volumes*, Volume 32, Issue 2, July 1999, Pages 2598-2603.

LEVY, N., IV, M. and YOM-TOV, E. (2018) Modeling influenza-like illnesses through composite compartmental models, *Physica A*, 494 (2018) 288–293.

LI, Y., WANG, Z. and SONG, Y. (2006) Wireless Sensor Network Design for Wildfire Monitoring, Intelligent Control and Automation, 2006. WCICA *2006. The Sixth World Congress on, Volume*: 1, DOI: 10.1109/WCICA.2006.1712372

LOU, Y. and CHRISTOFIDES, P. D. (2003) Optimal Actuator/Sensor Placement for Nonlinear Control of the Kuramoto-Sivashinsky Equation, *IEEE Trans. on Control Systems Technology*, VOL. 11, NO. 5, September 2003.

MALLARDO, V. and ALIABADI, M.H. (2013) Optimal Sensor Placement for Structural, Damage and Impact Identification: A Review, *SDHM*, Vol.9, No. 4, pp. 287-323.

MANDEL, J., BENNETHUMA, L. S., BEEZLEY, J. D., COEN, J. L., DOUGLAS, C. C., KIM, M. and VODACEK, A. (2008), A wildland fire model with data assimilation, *Mathematics and Computers in Simulation*, Vol.79, (2008), pp. 584–606.

MARX, B., KOENIG D. and GEORGES, D. (2004) Optimal sensor and actuator location for descriptor systems using generalized gramians and balanced realizations, IEEE American Control Conference, Boston, USA, 2004.

MICHALSKA. H. and MAYNE, D. Q. (1995) Moving Horizon Observers and Observer-Based Control, *IEEE Transactions on Automatic Control*, VOL. 40, No. 6, JUNE 1995.

MOHD ALI J., HOANG, HA., HUSSAIN, M. A. and DOCHAIN, D. (2015) Review and classification of recent observers applied in chemical process systems, *Computers and Chemical Engineering* 76 (2015) 27–41.

MOSTAFAEIA, H. and MENTHB, M. (2018) Software-defined wireless sensor networks: A survey, *Journal of Network and Computer Applications*, 119 (2018) 42–56.

MUSKE, K. and RAWLINGS, J.B. (1995) Nonlinear receding horizon state estimation. In: Methods of Model-Based Control (R. Berber, Ed.). NATO-ASI Series. *Kluwer Press*. Dordrecht. Netherlands, 1995.

NGUYEN T., GEORGES, D. and TRAN T. Q. (2008) An Energy Approach to Optimal Selection of Controllers and Sensors in Power System, International Journal of Emerging Electric Power Systems, *Berkeley Electronic Press*, Vol. 9, 2008, hal-00370850 http://www.bepress.com/ijeeps/vol9/iss6/art2.

NGUYEN, Tri Van and GEORGES, D. and BESANCON, G. (2016) Optimal sensor location for overland flow network monitoring, 3rd Conference on Control and Fault-Tolerant Systems (SysTol 2016), Sep 2016, Barcelone, Spain. hal-01333742.

OGATA, K. (2010) Modern Control Engineering, 5th edition, Prentice Hall, 2010.

OGIE, R., SHUKLA, N. and HOLDERNESS, T. (2017) Optimal placement of water-level sensors to facilitate data-driven management of hydrological infrastructure assets in coastal mega-cities of developing nations, Sustainable Cities and Society · August 2017.

PARK, S., SEON, K. and XU, L., *et al* (2017) *Data Assimilation for Atmospheric, Oceanic and Hydrologic Applications*, Volume 3, Springer, 2017.

PHAM, V. T., GEORGES, D. and BESANCON, G. (2013) Receding Horizon Observer and Control for linear 2X2 hyperbolic systems of conservation laws, 2013 European Control Conference (ECC) July 17-19, 2013, Zürich, Switzerland.

PRIVAT, Y., TRELAT, E. and ZUAZUA, E. (2014) Optimal shape and location of sensors or actuators in PDE models, 2014 American Control Conference (ACC) June 4-6, 2014. Portland, Oregon, USA.

QI, J., SUN. K. and KANG, W. (2014) Optimal PMU Placement for Power System Dynamic State Estimation by Using Empirical Observability Gramian, *IEEE Trans. on Power Systems*, 2014.

RANGEGOWDA, P. H., VALLURU, J., PATWARDHAN, S. C. and MUKHOPADHYA, S. (2018) Simultaneous State and Parameter Estimation using Receding-horizon Nonlinear Kalman Filter, *IFAC PapersOnLine*, 51-18 (2018) 411–416.

RAWLINGS, J. B. and BAKSHIB, B. R. (2006) Particle filtering and moving horizon estimation, *Computers & Chemical Engineering*, Volume 30, Issues 10–12, 12 September 2006, Pages 1529-1541

SONG, Z., CHEN, Y.Q., SASTRY, C. R. and TAS, N. C. (2009) Optimal Observation for Cyber-physical Systems: A Fisher-information-matrix approach, Springer 2009.

SPINELLI, B., CELIS, L. E. and THIRAN, P. (2017) A General Framework for Sensor Placement in Source Localization, World Wide Web Conference, 2017.

SUMMERS, T. H. and LYGEROS, J. (2014) Optimal Sensor and Actuator Placement in Complex Dynamical Networks, 19th IFAC World Congress, *IFAC Proceedings Volumes*, Volume 47, Issue 3, 2014, Pages 3784-3789.

TANG, S. and MORRIS, K. A. (2017) Optimal Sensor Design for Infinite-Time Kalman Filters, 2017 IEEE 56th Annual Conference on Decision and Control (CDC) December 12-15, 2017, Melbourne, Australia.

TERZIS, A., ANANDARAJAH, A., MOORE, K. and WANG, I-J. (2006) Slip Surface Localization in Wireless Sensor Networks for Landslide Prediction, IPSN'06, April 19–21, 2006, Nashville, Tennessee, USA. Copyright 2006 ACM 1-59593-334-4/06/0004.

THURO, K., SINGER, J., FESTL, J., WUNDERLICH,P, T., WASMEIER, P., REITH, C., HEUNECK, O., GLABSCH, J. and SCHUBACK, S. (2017) New landslide monitoring techniques – developments and experiences of the alpEWAS project, *Journal of Applied Geodesy*, 2017, https://doi.org/10.1515/jag.2010.008.

UCINSKI, D. (2005) Optimal Measurement Methods for Distributed-Parameter System Identification. Boca Raton, FL: *CRC Press*, 2005.

WOUWER, A. Vande, POINT Nicolas, PORTEMAN, S. and REMY, M. (2000) An approach to the selection of optimal sensor locations in distributed parameter systems, *Journal of Process Control*, 10 (2000) 291-300. 29

ZAN, T., GUPTA, P., WANG, M., DAUWELS, J. and UKIL, A. (2018) Multi-Objective Optimal Sensor Placement for Low-Pressure Gas Distribution Networks, *IEEE SENSORS JOURNAL*, VOL. 18, No. 16, Aug. 15, 2018.

ZANNETTI, P. (1990) *Air Pollution Modelling. Theories, Computational Methods and Available Software*, Computational Mechanics Publications, Southampton, Boston, Van Nostrand Reinhold, New York, Springer, 1990.

ZHANG, C. and HADDADI, H. (2019) Deep Learning in Mobile and Wireless Networking: A Survey, *IEEE Communications Surveys & Tutorials, 2019*.

ZIO, E. (2018) The future of risk assessment, *Reliability Engineering & System Safety*, Volume 177, September 2018, Pages 176-190. 30